8-7-2008

B-Spline Boundary Element Method for Ships

Aditya Mohan Aggarwal
University of New Orleans

B-Spline Boundary Element Method for Ships

A Thesis

Submitted to the Graduate Faculty of the
University of New Orleans
in partial fulfillment of the
requirements for the degree of

Master of Science
in
Engineering
Naval Architecture and Marine Engineering

by

Aditya Mohan Aggarwal

B.S. University of New Orleans, 2006

August, 2008

Dedication

For their sacrifice, love and support, this thesis is dedicated to Shail, Archana and Yogendra. Their faith in my abilities has been the inspiration and driving force for all my accomplishments, past and present.

Acknowledgement

I wish to thank my advisor, Dr. Lothar Birk, Associate Professor of Naval Architecture and Marine Engineering at the University of New Orleans, who gave me an opportunity to do my graduate research work under his able and much sought-after mentorship. I have immensely benefited from his expertise in the field, and his guidance through the course of this thesis. This thesis would not have been complete without his expert advice and unfailing patience.

I am very grateful to Dr. William Vorus, Professor of Naval Architecture and Marine Engineering, and Dr. George Ioup, University Research Professor of Department of Physics, for their participation in my thesis. I would like to take this opportunity to also thank Dr. Jeffery Falzarano, now a professor at Texas A&M University, who motivated me towards research work during my undergraduate studies at the University of New Orleans.

This work was supported by the Louisiana Board of Regents Support Fund Research & Development Program.

And, last but not least, I would also like to express a special word of thanks to the present faculty and staff of the University of New Orleans. Their unselfish dedication, in the aftermath of Hurricane Katrina, has been invaluable to the UNO community as we recover and rebuild.

Table of Contents

List of Figures

Nomenclature

μ	doublet strength
Φ	total potential
ϕ	perturbation potential
$\phi^{(0)}$	zero order wave potential
$\phi^{(1)}$	first order wave potential
ϕ_∞	potential for the uniform onset flow
σ	source strength on the source surface
$\underline{A}$	vector A (underscore represents a vector)
$\underline{n_p}$	normal at point $\underline{\mathrm{P}}$
$\underline{p}$	point on the hull surface
$\underline{P_{ij}}$	hull surface vertices
$\underline{q}$	point on the source surface
$\underline{Q_{ij}}$	source surface vertices
$\underline{U_\infty}$	fluid onflow velocity (opposite of body velocity)
$\underline{v}$	velocity field
ζ	free-surface elevation
$\zeta^{(0)}$	zero order wave elevation
M	total number of vertices for the surface in v
N	total number of vertices for the surface in u
S_b	hull surface
S_{ij}	source strength vertices

U_b body velocity

$\underline{n}$ normal vector, $\begin{pmatrix} n_x \\ n_y \\ n_z \end{pmatrix}$

S_F free surface

Abstract

The development of a three dimensional B-Spline based method, which is suitable for the steady-state potential flow analysis of free surface piercing bodies in hydrodynamics, is presented.

The method requires the B-Spline or Non Uniform Rational B-Spline (NURBS) representation of the body as an input. In order to solve for the unknown potential, the source surface, both for the body as well as the free surface, is represented by NURBS surfaces. The method does not require the body surface to be discritized into flat panels. Therefore, instead of a mere panel approximation, the exact body geometry is utilized for the computation. The technique does not use a free surface Green's function, which already satisfies the linear free surface boundary conditions, but uses a separate source patch for the free surface. By eliminating the use of a free surface Green's function, the method can be extended to considering non-linear free surface conditions, thus providing the possibility for wave resistance calculations.

The method is first applied to the double body flow problem around a sphere and a Wigley hull. Some comparisons are made with exact solutions to validate the accuracy of the method. Results of linear free surface conditions are then presented.

Keywords: potential theory, steady-state flow, B-Spline, NURBS, double body flow, linear free surface conditions

Chapter 1

Introduction

Naval architects have always been interested in analyzing the fluid motion around ships as they move forward in a steady-state on the calm free water surface, thus generating a wave field behind them. For a range of computations in marine hydrodynamics, the fluid flow is considered to be inviscid, incompressible and irrotational. With the condition of irrotationality in place, the velocity field $\underline{v}$ in the fluid domain can be described by a potential function Φ [16].

$$\underline{v} = \underline{\nabla}\Phi \tag{1.1}$$

From the conservation of mass and the condition of an incompressible fluid follows the Laplace equation [16].

$$\nabla^2\Phi = 0 \tag{1.2}$$

The application of Laplace's equation in marine hydrodynamics ranges from the most basic fluid flow past a deeply submerged cylinder to the most complex flow past a ship excited by waves [16]. Earlier solutions for potential flows in ship hydrodynamics involved methods that were based on the strip theory [4]. With the assumption that the ship is a slender body, the analysis was conducted in two dimensions and integrated over the length of the ship. But as significant progress was made to accurately predict ship motions, three dimensional methods that eliminated the assumption of slenderness were implemented. In the last decade, advancements in computer technology have further motivated researchers to develop many different classes of three-dimensional techniques for improved numerical analysis of ship motions.

A majority of three dimensional analysis techniques in marine hydrodynamics use the boundary element method. As the name suggests, the solution to the problem in a domain is

defined by conditions on its boundaries. These conditions need not be solved on other points in the domain as they are specific boundary conditions. Hence, it tremendously reduces the computation domain. For marine hydrodynamics, we are specifically interested in the fluid properties at the boundaries, such as fluid pressure on the hull and the free surface elevation. Panel methods are a subgroup of boundary element methods, and a highly utilized method for problems in hydrodynamics. Like all other boundary element methods, the analysis domain for panel methods comprises only the boundary surfaces of the problem. The boundary surfaces are discretized using a grid. The elements of the grid are referred to as "panels".

1.1 Panel Methods

Panel methods can be formulated in many ways, but the pioneering work of Hess and Smith [7] was the first truely practical method. More will be discussed in the next section. A brief overview of the general formulation for the panel method is provided in this section. For a more elaborate explanation, the reader is referred to Katz and Plotkin [11], or any other computational fluid dynamics text book.

Before we go any further, it is important to specify the coordinate system that has been used for this work. Figure 1.1 represents the coordinate system that is consistent with the theory, formulation and the results for the current work. The body is located at (0,0,0), with a forward speed in the positive x-direction. Hence, the onflow fluid velocity U_∞ can be considered to be opposite to the body velocity.

$$\underline{U}_\infty \;=\; (-U_b, 0, 0)^T \tag{1.3}$$

For the free-surface problem, the fluid surface is located at z=0. Symmetry of the body along the x-axis and the y-axis, wherever applicable, has been exploited.

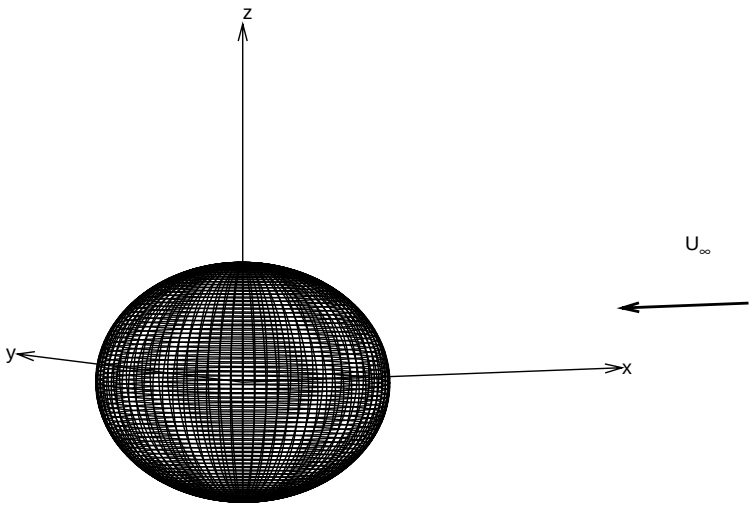

Figure 1.1: Coordinate system

As mentioned earlier, the Laplace's equation is extensively used in marine hydrodynamics. The total potential, Φ, for an irrotational fluid satisfies the Laplace's equation everywhere in the fluid domain. The most potent feature of the Laplace's equation is its linearity, which allows us to build up the complete solution out of simple elements. Instead of solving for the velocity field, a vector, we only need to solve for the potential, which is a scalar quantity. Boundary conditions are specified in order to determine a unique solution for the potential. As an example, the following boundary conditions have to be satisfied for a deeply submerged body.

$$\frac{\partial \Phi}{\partial n} = 0 \qquad \text{on } S_b \quad \text{body surface} \tag{1.4}$$

$$\lim_{r \to \infty} \nabla \Phi = \underline{U}_\infty \qquad \text{on } S_\infty \quad \text{far field} \tag{1.5}$$

The former condition, known as the rigid body condition, makes sure that there is no fluid flow through the body surface S_b. And the latter ensures that the effect of the body is eliminated far away from the body S_∞. Hence, far away from the body, the gradient of the potential would yield a velocity that is equal to the onflow fluid velocity.

As the analysis will only take surfaces into consideration, the aim is that the flow potential throughout the fluid domain should be expressed in terms of the surface that bounds the flow field. This is achieved by utilizing Green's Theorem, which converts the volume integral for the potential into a surface integral [16].

$$\iiint_V \left[\phi_2 \nabla^2 \phi_1 - \phi_1 \nabla^2 \phi_2\right] dV \;=\; \iint_S \left[\phi_2 \frac{\partial \phi_1}{\partial n} - \phi_1 \frac{\partial \phi_2}{\partial n}\right] dS \tag{1.6}$$

ϕ_1 and ϕ_2 are two potentials. We select $\phi_1 = \frac{-1}{4\pi r}$ and $\phi_2 = \phi$. Both potentials satisfy the Laplace's equation. r is the distance between any point $\underline{p} = (x, y, z)^T$ on the surface and a "source/sink" at the location $\underline{q} = (\xi, \eta, \zeta)^T$. Therefore,

$$\phi_1 = \frac{-1}{4\pi r} = \frac{-1}{4\pi\sqrt{(x-\xi)^2 + (y-\eta)^2 + (z-\zeta)^2}} \tag{1.7}$$

After some mathematical manipulation [11], the total potential $\Phi(\underline{p})$ at any point $\underline{p}$ within the fluid domain can be given by

$$\Phi(p) \;=\; \iint_{S_b} \sigma \left(-\frac{1}{4\pi r}\right) dS - \iint_{S_b} \mu \frac{\partial}{\partial n}\left(-\frac{1}{4\pi r}\right) dS + \phi_\infty(\underline{p}) \tag{1.8}$$

The first integral represents the potential due to a source distribution of strength σ and the second term is a *doublet* distribution. The latter is required for lifting surfaces only, and μ has been set equal to zero in the current work.

As the point $\underline{p}$ on the surface approaches the "sink", the term $\frac{1}{r}$ within the surface integral approaches infinity. Thus, the source and doublets are also known as *singularities*.

Applying the body boundary condition to the external flow potential, given by equation (1.8), yields a *Fredholm Integral Equation of the Second Kind* [3].

$$-\frac{1}{2}\sigma(\underline{p}) \;+\; \iint_{S_b} \sigma(\underline{q}) \frac{\partial}{\partial n_q}\left(-\frac{1}{4\pi r}\right) dS(\underline{q}) \;=\; \underline{n}_p^T \underline{U}_\infty \tag{1.9}$$

For a conventional panel method, the body surface is discretized into n panels. The source strength distribution over each panel can be constant, linear or of higher order. There are collocation points on the body surface, usually at the center of each panel, where the body boundary condition is solved. Hence, equation (1.9) is solved at each collocation point,

taking into consideration the effect of the singularity distribution over all the panels. The effect of the panel on which the collocation point is located is known as the *self* term.

Equation (1.9) turns into a set of n linear equations with n unknown coefficients σ. If we assume constant source strength distribution over the panels, we can move σ out of the surface integral. The unknown coefficients σ are the n unknown source strength values for the panels on the body.

$$\sum_{i=1}^{n}\left[-\frac{1}{2}\sigma(\underline{p}_i) + \sum_{j=1}^{n}\sigma(\underline{q}_j)\frac{\partial}{\partial n_{p_i}}\iint_{S_j}\left(-\frac{1}{4\pi r(\underline{p}_i,\underline{q})}\right)dS_j\right] = \sum_{i=1}^{n}\underline{n}_{p_i}^{T}\underline{U}_{\infty} \tag{1.10}$$

Once the set of equations are solved to compute the unknown source strength σ, we can compute the potential ϕ. Since we do not directly compute the potential, it is also known as the *indirect* method. The potential can be obtained by an additional integration of the source strength over the body surface.

$$\phi(\underline{p}) = \iint_{S_b}\sigma\left(\frac{-1}{4\pi r}\right)dS \tag{1.11}$$

Now the flow properties like the velocity field and pressure coefficient can be computed over the body surface.

Equation (1.9) is the *indirect* method. Another form of that equation is given by equation (1.12), known as the *direct* method. Here the potential is directly computed, and hence, there is no need for an additional integration.

$$-\frac{1}{2}\phi(\underline{p}) + \iint_{S_b}\phi(\underline{p})\frac{\partial}{\partial n_p}\left(-\frac{1}{4\pi r}\right)dS(\underline{q}) = \iint_{S_b}\underline{n}_p^{T}\underline{U}_{\infty}\left(-\frac{1}{4\pi r}\right)dS(\underline{q}) \tag{1.12}$$

1.2 Research Background

An in-depth understanding of the past research work is necessary to appreciate what has already been achieved in this area, and to better comprehend the current work. Although invaluable, a comprehensive overview of the past research in this area is beyond the scope of this document. For those interested, Atkinson [1] offers an elaborate review of panel methods. This section is only meant to provide the reader with a brief overview of the development of the panel method since its inception.

The first successful implementation of the panel method to solve potential flow about

three dimensional bodies is credited to Hess and Smith [7]. Their work is based on distributing sources on the body surface, and obtaining the actual values for these sources that would help satisfy the body boundary condition of zero normal velocity at the surface. As discussed in the previous section, satisfying the condition results in a *Fredholm Integral Equation of the Second Kind*.

For distribution of sources, the body surface is discritized into quadrilateral elements and each element has a constant source value. The discritization of the surface into flat elements results in an approximation of the body, and the flow around it. Compared to more elaborate and computationally expensive techniques, this method provides an efficient and accurate solution. The method is beneficial for comparative analysis of different body shapes. Of course, to improve the approximation, the number of elements can be increased. However, it would result in an increase in the number of sources, and hence, an increase in the computation time. The strength of the method is its simplicity and ease of implementation.

Propelled by the work of Hess and Smith, panel methods have since evolved. Success of Hess and Smith's approach led the world of numerical potential flow analysis into a period that saw development of different versions of panel methods. Researchers developed variations of the method that are catogorized as lower or higher order panel methods. Johnson [10] and Kehr et al. [12] use a linear function to define the source over each panel. The constant and linear source distribution constitutes the lower order methods. The higher order methods define the surface geometry and the source distribution with quadratic or higher order functions [4]. Hess later developed a higher order method that makes use of curved panels of second degree with linearly varying source density [6]. Hsin et al. presented a higher order method that uses B-Splines to define the body geometry and the source solution [8]. For the same computation time, Hsin et al. claim the method to be more accurate than the lower order methods. Refer to Kouh and Suen for a brief list of lower and higher order methods [20].

Dawson was the first researcher to bring to light the use of panels on the free surface for computation of steady-state free surface waves [19]. His work relating to steady-state potential flow, on or near the free surface, focuses on solving for the source density on the quadrilateral panels for the body surface as well as the free surface [5]. Panels on the free-surface increases the computation time tremendously due to the large domain that needs to be covered on the free-surface. In order to reduce computation for free surface problems, researchers developed methods that utilize B-Spline approach along with a transient Green function [4]. Maniar used B-Splines to developed a higher order method and applied it to the radiation-diffraction problem [15]. The use of a free surface Green's function restricts the solution to that for linear free surface conditions only.

Marine hydrodynamists are among the very few researchers that have to deal with the issue of free surface effects, and probably the only ones using potential methods. Solving the complete non-linear free surface conditions, in the most efficient manner, still remains a challenge.

Chapter 2

The Method

As discussed in the previous chapter, many different variations of numerical procedures have been implemented in order to perform efficient and accurate three dimensional analysis. The motivation of this work is no different. However, our underlying goal is to conduct the analysis on the original geometry of the body rather than on its approximation, and also to be able to compute the flow properties at any arbitrary point on the body surface.

Most computer aided design softwares use a NURBS or B-Spline description to accurately represent body surfaces. Equation (2.1) describes a general B-spline surface [18] .

$$S(u,v) \;=\; \sum_{i=0}^{n}\sum_{j=0}^{m} P_{ij} N_{ip}(u) N_{jq}(v) \tag{2.1}$$

where, P_{ij} are the vertices, and, N_{ip} and N_{jq} are the basis functions. The basis functions are based on their respective knot vectors in u and v.

This work is based on exploiting the B-Spline description of the body to generate an offset B-Spline source surface. The source strength over the entire source surface also uses a B-Spline distribution. The potential due to the source strength over the source surface satisfies the Laplace's equation, as required by the potential theory. Forthcoming section discusses more about the body surface, the source surface and the source strength distribution. And the later sections in this chapter will discuss the formulation of the boundary conditions for the current work.

It is assumed that the reader has basic knowledge of parametric surfaces. Otherwise, Piegl and Tiller is the most comprehensive source on NURBS [18]. Nowacki, Bloor and Oleksiewicz is also an excellent source for review [17].

2.1 Surfaces and the Source Strength

As discussed in the previous chapter, the total potential Φ, after setting *doublet* distribution equal to zero, can be given by

$$\Phi(\underline{p}) \;=\; \iint_{S_b} \sigma \left(-\frac{1}{4\pi r}\right) dS + \phi_\infty(\underline{p}) \tag{2.2}$$

In equation (2.2), the sources have been distributed over the body surface, and hence, the integration of the first term ϕ_1 is performed over the body surface S_b. In general, the integration is performed over the surface where the sources have been distributed.

For the evaluation of the integral expression, traditional numerical methods in potential flow problems face a common difficulty of evaluating the *self* term. The integral expression possess singularity of the integral equation kernel at points where the distance r becomes zero. Physically, it means that the effect of a point on its own self is being calculated. The presence of such a singularity makes its difficult to numerically evaluate the integral.

To deal with this difficulty of numerical evaluation of the integral expression, a source surface is generated that does not overlap the body surface. This de-singularization shifts the source surface away from the collocation points, hence, converting a singular integral expression into a non-singular expression. The degree of difficulty faced to integrate the latter expression is assumed to be much less than that for the former.

The source strength distribution over the source surface also utilizes a B-Spline description. Therefore, the body surface, the source surface and the source strength, are all B-Spline surfaces. In the current work the standard definition of these B-Spline surfaces, also known as the tensor product surfaces, are given by

$$\text{Source Strength,} \quad \sigma\,(u,v) \;=\; \sum_{i=1}^{N_s}\sum_{j=1}^{M_s} S_{ij} N_{ik_s}\,(u)\, N_{jl_s}\,(v) \tag{2.3}$$

$$\text{Hull Surface,} \quad \underline{p}\,(u_p,v_p) \;=\; \sum_{i=1}^{N_p}\sum_{j=1}^{M_p} \underline{P}_{ij} N_{ik_p}\,(u_p)\, N_{jl_p}\,(v_p) \tag{2.4}$$

$$\text{Source Surface,} \quad \underline{q}\,(u,v) \;=\; \sum_{i=1}^{N_q}\sum_{j=1}^{M_q} \underline{Q}_{ij} N_{ik_q}\,(u)\, N_{jl_q}\,(v) \tag{2.5}$$

where, $S_{ij}, \underline{P}_{ij}$ and $\underline{Q}_{ij}$ denote the vertices of source strength, body surface and source surface, respectively. N and M, for the summation, are the total number of vertices in the u and v direction. N_{ik} and N_{jl} represents the basis functions associated with the i^{th} and j^{th}

vertex, and are of the order k and l. The second level subscripts of s, p and q, represent the source strength, body surface and source surface, respectively. Note that the basis functions for the source surface and the source strength are based on the same knot vectors in u and v. Conventionally, the first vertex is denoted by the subscript 0, but in the current formulation the first vertex has been assigned the subscript 1.

It is worth summarizing that the surfaces are represented by vectors, and the source strength is a scalar quantity. The coordinate system is stationary to the hull, z axis points vertically upwards, with z=0 at the calm free water surface.

As mentioned previously, there is a source strength distribution over the source surface. Like any B-Spline surface, this source distribution has its source strength vertices, S_{ij}. These source strength vertices are scalar quantities and not geometric points. Similar to the manner in which a B-Spline surface is computed, the source strength σ can be computed anywhere on the source surface by the source strength vertices, S_{ij} and the source strength basis functions. As mentioned earlier, the basis functions are based on the same knot vectors for the source surface as well as the source strength. Hence, allowing the integration of the source strength over the entire source surface without undergoing a variable transformation for the integration limits.

Figure 2.1 summarizes the transformation cycle that the source surface has to undergo in order to compute the source strength distribution. The source surface in the global coordinate system resembles the hull surface, but does not overlap it. It order to proceed with the B-Spline computation, the source surface has to be transformed from the global system of xyz variables to parametric variables (u,v), as shown by figure 2.1(a). Both parametric variables have a minimum value of 0 and a maximum value of 1. The magnitude of the source strength over the entire source surface is calculated in the parametric domain, figure 2.1(b). Finally, the source strength distribution is transformed back from the parametric domain to the global domain, as shown in figure 2.1(c). Hence, representing the source strength distribution over the actual source surface in the global xyz system.

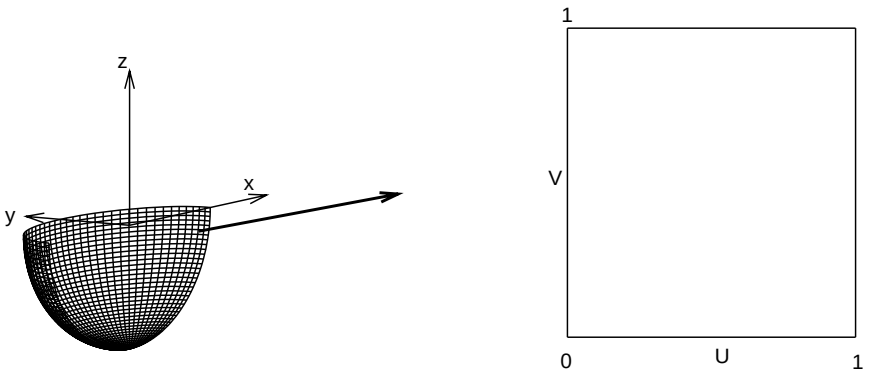

(a) Global to parametric transformation of the source surface

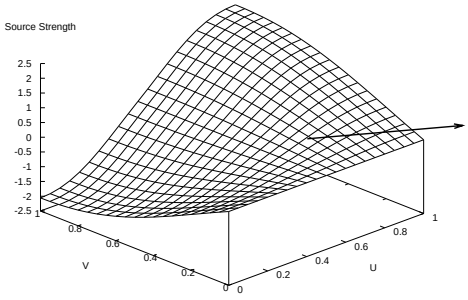

(b) Source strength on parametric scale

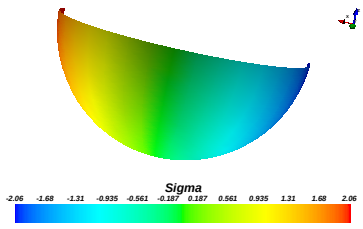

(c) Source strength on global scale

Figure 2.1: Source surface transformation from global to parametric domain. And re-transformation of the source strength distribution over the source surface from parametric to global domain.

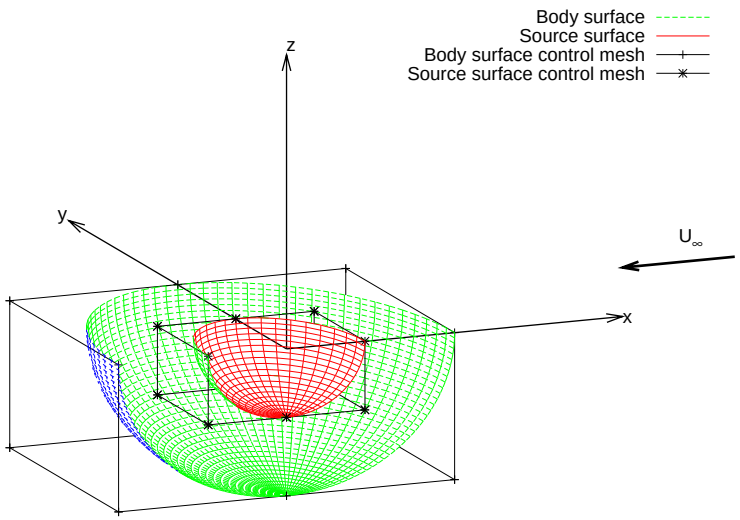

Figure 2.2: Body surface and the source surface (offset has been exaggerated)

Back to the offset of the source surface, figure 2.2 provides a better insight on the arrangement of the source surface and the hull surface. The hull surface is a B-spline surface, and its vertices are denoted by $\underline{P}_{ij}$. B-Spline data for the hull surface can be obtained from any computer aided design software used in naval architecture, e.g. Rhinoceros. Like the hull surface, the source surface is also a B-Spline surface. However, it is shifted away from the hull surface by a distance that is dependent on α. The data for the hull surface is already available, therefore, for representing the source surface it is convenient to use the same vertices and basis functions. The source surface has been shifted away from the hull surface, hence, the vertices for the two surfaces are not the same anymore. The source surface vertices are represented by $\underline{Q}_{ij}$. The vertices for the source surface are given by equation (2.6). However, it is important to note that using the factor α to shift the source surface is a simplified method, and can only be used for simple shapes like a sphere, wigley hull etc. Since the expression simply contracts the source surface toward the origin, it is necessary that the coordinate system be centered at the calm water line, z=0. An example where this might not work as desired is the region of the bulbous bow, where the source surface when shrunk toward the origin would actually intersect the hull surface. For such

cases, the computer aided design software can easily generate an offset surface that can be used as the source surface.

$$\underline{Q}_{ij} \;=\; \alpha \underline{P}_{ij} \tag{2.6}$$

where, both, the body vertices $\underline{P}_{ij}$, and the source surface vertices $\underline{Q}_{ij}$ are vectors.

It is important to explicitly state that there are no "panels" in the current work. The source surface is a B-Spline surface and does not need discretization, as opposed to the conventional panel methods where the body is discretized into smaller panels and a source strength is assigned to each panel. Hence, the current work is based on a paneless method.

2.2 Body Boundary Condition

The hull surface boundary condition requires that there is no normal flow of fluid through the body surface.

$$\frac{\partial \Phi}{\partial n} \;=\; 0 \tag{2.7}$$

As discussed in the previous chapter, the total potential, $\Phi(\underline{p})$, at any point can be given by

$$\Phi(\underline{p}) \;=\; \underline{p}^T \underline{U}_\infty \;+\; \iint\limits_{S_q} \sigma \left(\frac{-1}{4\pi r\left(\underline{p}, \underline{q}\right)} \right) dS_q \;=\; \underline{p}^T \underline{U}_\infty \;+\; \phi \tag{2.8}$$

In equation (2.8), ϕ is also known as the *perturbation potential*, and it represents the disturbance of the parallel flow due to the presence of the body. Therefore, the hull surface boundary condition can be re-arranged as

$$\underline{n}_{\underline{p}}^T \cdot \iint\limits_{S_q} \sigma \underline{\nabla} \left(\frac{-1}{4\pi r\left(\underline{p}, \underline{q}\right)} \right) dS_q \;=\; -\underline{n}_{\underline{p}}^T \cdot \underline{U}_\infty \tag{2.9}$$

where, $\underline{p} \neq \underline{q}$ because $\underline{p} \in S_b$ and $\underline{q} \in S_q$

Re-arranging the left hand side by substituting the B-Spline representation of σ, and transforming the integration to the parametric domain, we obtain

$$\underline{n}^T \cdot \iint\limits_{S_q} \sigma \underline{\nabla} \left(\frac{-1}{4\pi r\left(\underline{p}, \underline{q}\right)} \right) dS_q \;=$$
$$\underline{n}^T \cdot \iint\limits_{S_q} \left[\sum_{i\,=\,1}^{N_s} \sum_{j\,=\,1}^{M_s} S_{ij} \cdot N_{ik_s}(u) N_{jl_s}(v) \right] \cdot \underline{\nabla} \left(\frac{-1}{4\pi r\left(\underline{p}, \underline{q}\right)} \right) \|\underline{q}_u \times \underline{q}_v\| du dv \tag{2.10}$$

where, $\|\underline{q}_u \times \underline{q}_v\|$ is the *Jacobian of the variable transformation* ($dS_q \;=\; \|\underline{q}_u \times \underline{q}_v\| \; dudv$).

The gradient of the potential ϕ, yields the following result

$$\underline{\nabla}\left(\frac{-1}{4\pi r\left(\underline{p},\underline{q}\right)}\right) = \begin{pmatrix} \frac{\partial}{\partial x}\left(\frac{-1}{4\pi r\left(\underline{p},\underline{q}\right)}\right) \\ \frac{\partial}{\partial y}\left(\frac{-1}{4\pi r\left(\underline{p},\underline{q}\right)}\right) \\ \frac{\partial}{\partial z}\left(\frac{-1}{4\pi r\left(\underline{p},\underline{q}\right)}\right) \end{pmatrix} = \frac{1}{4\pi r^3\left(\underline{p},\underline{q}\right)}\begin{pmatrix} (p_x - q_x) \\ (p_y - q_y) \\ (p_z - q_z) \end{pmatrix} \tag{2.11}$$

Substituting the gradient of the potential ϕ from equation (2.11) into (2.10) produces the following

$$\underline{n}^T \cdot \iint_{S_q} \sigma \underline{\nabla}\left(\frac{-1}{4\pi r\left(\underline{p},\underline{q}\right)}\right) dS_q \; = \iint_{S_q} \left[\sum_{i=1}^{N_s}\sum_{j=1}^{M_s} S_{ij} \cdot N_{ik_s}(u) N_{jl_s}(v)\right] \left[\frac{1}{4\pi r^3} \cdot \underline{n}^T \begin{pmatrix} p_x - q_x \\ p_y - q_y \\ p_z - q_z \end{pmatrix}\right] \|\underline{q}_u \times \underline{q}_v\| dudv \tag{2.12}$$

Equation (2.12) is the normal velocity of the source surface at a collocation point $\underline{p}$ on the hull surface. It is computed by integrating the sum of the product of all the basis functions with their respective vertices, over the entire source surface. We know, through basic calculus, that the integration of a sum of functions over a limit is equivalent to the sum of the individual functions integrated over the same limit.

$$\left(\iint \left[f_1 + f_2 + f_3 \ldots\right] dudv = \iint f_1 dudv + \iint f_2 dudv + \iint f_3 dudv \ldots\right)$$

We also know that the vertices of a B-Spline surface are not a function of the parameters u and v. Therefore, the source strength vertices S_{ij} are constants with respect to the integration variables u and v. Hence, equation (2.12) can re-written as

$$\underline{n}^T \cdot \iint_{S_q} \sigma \underline{\nabla} \left(\frac{-1}{4\pi r\left(\underline{p},\underline{q}\right)} \right) dS_q \;=$$

$$\sum_{i=1}^{N_s} \sum_{j=1}^{M_s} S_{ij} \iint_{S_q} N_{ik_s}(u) N_{jl_s}(v) \cdot \left[\frac{1}{4\pi r^3} \cdot \underline{n}^T \begin{pmatrix} p_x - q_x \\ p_y - q_y \\ p_z - q_z \end{pmatrix} \right] \|\underline{q}_u \times \underline{q}_v\| du dv \quad (2.13)$$

We require a set of linear equations to solve for the source strength S_{ij}. We need a set of $N_s \times M_s$ linear equations since that is the total number of unknown source strength vertices. The total number of basis functions for the source surface is also $N_s \times M_s$. Note that even though equation (2.13) has been discretized into $N_s \times M_s$ elements, but it is still exact and continuous. All the vertices and basis functions together make up the exact source surface. In order to generate a set of linear equations we need to select collocation points equal to the number of basis functions for the source surface. Therefore, we must select $N_s \times M_s$ collocation points on the hull surface to satisfy the body boundary condition.

It is important to strategically locate the collocation points on the hull. The source strength σ on the source surface will be expressed as a B-Spline surface, and would be dependent on the values of the source strength vertices S_{ij} and its set of basis functions. To ensure that the scalar source strength can be integrated over the complete source surface, we had used the same knot vectors for the source surface and the source strength. Therefore, they both have the same basis functions as well. For a simple body geometry the hull surface and the source surface have been offset by a distance that is dependent on the value of α. The source surface can use the same basis functions as the body surface. Therefore, for simple bodies the body surface, the source surface and the source strength share the same set of basis functions.

The body boundary condition has to be satisfied everywhere on the body, e.g. at all the collocation points. The following expression is a set of $N_s \times M_s$ linear equations, with $N_s \times M_s$ components in each equation, and is solved at the collocation points.

$$\sum_{i=1}^{N_s} \sum_{j=1}^{M_s} S_{ij} \iint_{S_q} N_{ik_s}(u) N_{jl_s}(v) \left[\frac{1}{4\pi r^3(\underline{p}_m,\underline{q})} \cdot \underline{n}_m^T \begin{pmatrix} p_{x_m} - q_x \\ p_{y_m} - q_y \\ p_{z_m} - q_z \end{pmatrix} \right] \|\underline{q}_u \times \underline{q}_v\| du dv \;=$$

$$- \left(\underline{n}_m^T \underline{U}_\infty\right) \quad (2.14)$$

where, m = 1, 2, ... $N_s \times M_s$

Equation (2.14) gives us a set of $N_s \times M_s$ linear equations, which needs to be solved in order to determine the coefficients. The coefficients, S_{ij}, are the source strength vertices. It is worth mentioning again that the source surface vertices $\underline{Q}_{ij}$, and the source strength vertices S_{ij}, are different. The former being a vector and the later a scalar.

In case of a double body flow problem, solving equation (2.14) to determine the source strength at the control points suffices. We can now compute the total potential Φ since the source strength is just another NURBS surface, and knowing S_{ij} and the basis functions is enough to compute the value of the source strength everywhere on the source surface. The velocity field is obtained by taking the gradient of the total potential Φ.

But, if the body is situated on or near the free surface and the desired results include the effect of the free surface due to the fluid-body interaction, it is necessary to solve additional conditions.

2.3 Free-Surface Conditions

The subject of water waves, when dealt alone, is already considered one of the most complex physical problems in nature. The presence of a body within the water waves ramifies this complexity [22]. Any work aimed at solving the non-linear free surface elevation problem has to be first successfully solved for the linearized free surface conditions. The free surface boundary conditions, for the problem on our hands, pose a couple of major difficulties. Firstly, they are non-linear in nature, and secondly, the boundary conditions on the free surface need to be satisfied on a surface whose location is not known beforehand. The latter makes the solution to the boundary conditions implicit in nature.

Traditionally, researchers have used the *Neumann-Kelvin Linearization* for transforming the non-linear wave elevation problem into a linear problem. The aforesaid assumes the undisturbed parallel on-flow with no waves as the basic solution to the problem.

$$\phi^{(0)} = -U_b x \tag{2.15}$$

$$\zeta^{(0)} = 0 \tag{2.16}$$

where, $\phi^{(0)}$ and $\zeta^{(0)}$ are the zero order wave potential and wave elevation, respectively.

Linearity of the Laplace's equation allows the superimposition of two or more simple solutions to form a new solution for potential flows. Equations (2.17) and (2.18) express the exact solution for the velocity potential Φ and the wave elevation ζ as a sum of functions with rapidly decreasing values [3]. To linearize, we truncate the sum after the first order terms. The second and higher order terms are ignored, and it is assumed that their contributions are negligible. This linearization is practical for free surface flows as long as the wave steepness is not too large.

$$\Phi = \phi^{(0)} + \varepsilon\phi^{(1)} + \varepsilon^2\phi^{(2)} + \dots \tag{2.17}$$

$$\zeta = \zeta^{(0)} + \varepsilon\zeta^{(1)} + \varepsilon^2\zeta^{(2)} + \dots \tag{2.18}$$

We require two conditions to successfully compute the unknown free surface potential, at an unknown free surface elevation. These two are the *dynamic* and the *kinematic* boundary conditions [16]. The former uses the Bernoulli's equation ensuring that the pressure at the free surface is equal to the atmospheric pressure at all times. The latter condition imposes a restriction on the movement of the water particles, allowing them to only move tangentially to the free surface. The water particle velocity normal to the free surface is zero.

The following are the two conditions that the velocity potential Φ must satisfy at the free surface [5].

$$\textit{Dynamic}, \qquad \frac{1}{2}\left[\Phi_x^2 + \Phi_y^2 + \Phi_z^2 - U_\infty^2\right] + gz \;=\; 0 \qquad \text{on} \quad z = \zeta \tag{2.19}$$

$$\textit{Kinematic}, \qquad -\zeta_x \Phi_x - \zeta_y \Phi_y + \Phi_z \;=\; 0 \qquad \text{on} \quad z = \zeta \tag{2.20}$$

Utilizing the *Neumann-Kelvin Linearization* from equations (2.15) and (2.16), the two boundary conditions can be linearized and expressed as

$$\textit{Linear Dynamic}, \qquad -U_b \phi_x^{(1)} + g\zeta^{(1)} \;=\; 0 \qquad \text{on} \quad z = 0 \tag{2.21}$$

$$\textit{Linear Kinematic}, \qquad \zeta_x^{(1)} U_b + \phi_z^{(1)} \;=\; 0 \qquad \text{on} \quad z = 0 \tag{2.22}$$

Equations (2.22) and (2.21) can be further combined. Take the x-derivative of the *dynamic* boundary condition and re-arrange the terms.

$$\zeta_x^{(1)} = \frac{U_b}{g} \phi_{xx}^{(1)} \tag{2.23}$$

Substituting equation (2.23) into equation (2.22), yields the following *Combined Linear Free-surface Boundary Condition* [19] [5] [2]. This needs to be solved at the zero order wave elevation, z=0.

$$U_b^2 \phi_{xx}^{(1)} + g\phi_z^{(1)} \;=\; 0 \tag{2.24}$$

Now that we have the *Combined Linear Free-surface Boundary Condition*, we need to formulate the set of linear equations that need to be solved at the collocation points on the free surface. It must be explicitly mentioned that, just like the hull surface, a separate source surface is generated for the free surface. The free surface and its source surface are both B-Spline surfaces. The free surface source surface is shifted upwards, in order to eliminate the singularity.

As metioned earlier, the zero order potential $\phi^{(0)}$ is the undisturbed parallel fluid onflow. The first order potential $\phi^{(1)}$ represents the disturbance caused by the body and is given by

$$\phi^{(1)} = \phi \tag{2.25}$$

The first and the second order x-derivates of the first order potential yields the following

$$\phi_x^{(1)} = \phi_x \tag{2.26}$$
$$\phi_{xx}^{(1)} = \phi_{xx} \tag{2.27}$$
$$\phi_z^{(1)} = \phi_z \tag{2.28}$$

Hence, by substituting the definition of *perturbation potential* ϕ in equations (2.27) and (2.28), and combining them with equation (2.24), the *Combined Linear Free-surface Boundary Condition* can be written as

$$U_b^2 \iint\limits_{S_F+S_b} \sigma(\underline{q}) \frac{\partial^2}{\partial x^2}\left(\frac{-1}{4\pi r}\right) dS_q \; + \; g \iint\limits_{S_F+S_b} \sigma(\underline{q}) \frac{\partial}{\partial z}\left(\frac{-1}{4\pi r}\right) dS_q \; = \; 0 \tag{2.29}$$

From equation (2.11), we can deduce

$$\frac{\partial}{\partial x^2}\left(\frac{-1}{4\pi r}\right) \; = \; \frac{1}{4\pi}\left(\frac{-3(p_x - q_x)^2}{r^5} \; + \; \frac{1}{r^3}\right) \tag{2.30}$$
$$\frac{\partial}{\partial z}\left(\frac{-1}{4\pi r}\right) \; = \; \frac{1}{4\pi}\frac{(p_z - q_z)}{r^3} \tag{2.31}$$

Replacing the second x-derivative and the z-derivative of ϕ in equation (2.29), substituting the description of source strength σ, and transferring it into the parametric domain, we get

$$U_b^2 \iint\limits_{S_F+S_b} \sum_{i=1}^{N_s+N_F} \sum_{j=1}^{M_s+M_F} S_{ij} N_{ik_s}(u) N_{jl_s}(v) \frac{1}{4\pi}\left(\frac{-3(p_x - q_x)^2}{r^5} \; + \; \frac{1}{r^3}\right) \|q_u \times q_v\| du dv$$
$$+ \; g \iint\limits_{S_F+S_b} \sum_{i=1}^{N_s+N_F} \sum_{j=1}^{M_s+M_F} S_{ij} N_{ik_s}(u) N_{jl_s}(v) \frac{1}{4\pi}\frac{(p_z - q_z)}{r^3} \|q_u \times q_v\| du dv \; = \; 0 \tag{2.32}$$

where, $N_F \times M_F$ is the total number of vertices for the free surface.

Just like the body boundary condition, we can interchange the integration and summation signs. The source strength vertices S_{ij} are not a function of u and v, and are treated as constants. The expression now becomes

$$\sum_{i=1}^{N_s+N_F}\sum_{j=1}^{M_s+M_F} S_{ij}\left(U_b^2\iint\limits_{S_F+S_b} N_{ik_s}(u)N_{jl_s}(v)\frac{1}{4\pi}\left(\frac{-3(p_x-q_x)^2}{r^5}+\frac{1}{r^3}\right)\|q_u\times q_v\|dudv\right.$$
$$\left.+\,g\iint\limits_{S_F+S_b} N_{ik_s}(u)N_{jl_s}(v)\frac{1}{4\pi}\frac{(p_z-q_z)}{r^3}\|q_u\times q_v\|dudv\right)\;=\;0 \tag{2.33}$$

Similar to the body boundary condition, the *Combined Linear Free-surface Boundary Condition* has to be satisfied everywhere on the free-surface, e.g. at all the $N_F M_F$ collocation points on the free-surface.

$$\sum_{i=1}^{N_s+N_F}\sum_{j=1}^{M_s+M_F} S_{ij}\left(U_b^2\iint\limits_{S_F+S_b} N_{ik_s}(u)N_{jl_s}(v)\frac{1}{4\pi}\left(\frac{-3(p_{x_m}-q_x)^2}{r^5(\underline{p}_m,\underline{q})}+\frac{1}{r^3(\underline{p}_m,\underline{q})}\right)\|q_u\times q_v\|dudv\right.$$
$$\left.+\;g\iint\limits_{S_F+S_b} N_{ik_s}(u)N_{jl_s}(v)\frac{1}{4\pi}\frac{(p_{z_m}-q_z)}{r^3(\underline{p}_m,\underline{q})}\|q_u\times q_v\|dudv\right)\;=\;0 \tag{2.34}$$

where, m $= N_sM_s+1, N_sM_s+2,\ldots N_sM_s+N_FM_F$

Note that m $= 1$ to N_sM_s refers to body surface collocation points, hence, m $= N_sM_s+1$ to $N_sM_s+N_FM_F$ are free-surface collocation points. It should also be evident that for each collocation point, whether its on the body surface or the free-surface, the effect of all the sources has to be considered. In equation (2.34) the effect of N_sM_s body source strength basis functions, and N_FM_F free-surface source strength basis functions has been included. Therefore, the total basis functions to be considered are N_s+N_F in the u direction and M_s+M_F in the v direction. At this point it is necessary to explicitly state that while considering the presence of free-surface, the system of equations for the body boundary condition has additional terms. These are due to the basis functions from the free-surface source strength. The expression to be solved for the body boundary condition in the presence of a free-surface is written as

$$\sum_{i=1}^{N_s+N_F}\sum_{j=1}^{M_s+M_F} S_{ij}\iint_{S_q} N_{ik_s}(u_s)N_{jl_s}(v_s)\left[\frac{1}{4\pi r^3(\underline{p}_m,\underline{q})}\cdot\underline{n}_m^T\begin{pmatrix} p_{x_m}-q_x \\ p_{y_m}-q_y \\ p_{z_m}-q_z \end{pmatrix}\right]\|\underline{q}_u\times\underline{q}_v\|dudv$$
$$= -\left(\underline{n}_m^T\underline{U}_\infty\right) \quad (2.35)$$

where, m = 1, 2, ... $N_s \times M_s$

Equations (2.34) and (2.35) form a system of linear equations with $N_sM_s+N_FM_F$ terms. Solving this system of linear equations will help us compute the source strength S_{ij} for all the source strength vertices for the body source strength, as well as on the free-surface source strength.

Once the values for the source strength vertices are known, the first order wave potential $\phi^{(1)}$ can be computed. And then, the *Linear Dynamic* boundary condition, equation (2.21), can be used to compute the first order wave elevation $\zeta^{(1)}$

$$\zeta^{(1)} = \frac{U_b}{g}\phi_x^{(1)} \quad (2.36)$$

In contrast to conventional panel methods, exact value for $\phi_x^{(1)}$ can be derived for equation (2.36). Conventional panel methods depend on numerical differentiation for computing ϕ_x.

2.4 Wave-making

It is of utmost importance that the waves which are generated as a result of the presence of the body at the free surface, must travel in the correct direction and be only present behind the body. The free surface problem on hand does not possess a unique solution [5]. In nature, waves only exist downstream of the body. However, if for some reason these waves are also generated upstream, they will satisfy the free surface conditions just as well as the downstream waves. There is no single correct solution to this problem, instead, it is in our hands to extract the correct solution from the many available solutions.

The correct application of the free surface conditions does not essentially ensure that the waves are only generated downstream [5]. In order to achieve the desirable solution, the set up of the problem has to be precise. In the past, researchers have used various techniques to ensure that the waves are only present downstream. It was suggested to force the first and second x-derivative of the pertubation potential ϕ to zero [2]. In a very well known research survey, Yeung mentioned the application of "asymptotic conditions", where the pertubation potential upstream and downstream has been described differently [22].

One of the more common method is the collocation point shift technique. For conventional panel methods the desired wave system is achieved by shifting the free surface collocation points upstream. The degree of shift can vary anywhere between 25% and 100% of the panel length [3]. Since the collocation points are the center of the panels that comprise the free surface, this essentially results in an upstream shift of the free surface domain. As a result, waves are only generated downstream of the body. The current work uses a variation of the collocation point shift method.

In the present work, the source surface for the free surface is not made up of panels [5] or point sources [9], but is a B-Spline surface. Being a B-Spline surface, the source surface is exact and continuous. The collocation points are selected points on the free surface domain where the free surface boundary conditions are satisfied. It is important to understand at this point that even though the number of source strength vertices are equal to the number of collocation points, the relationship between their respective positions is not the same as in a conventional panel method. In a conventional method, originally the sources are right above the collocation points, and later, they are shifted upstream. But, in the present work, the collocation points lie within the boundaries of the source surface in the xy plane. And even though we are just solving for the source strength values at the source strength vertices S_{ij}, the effect of the complete free surface source surface is taken into account. Therefore, a simple shift of all the collocation points would yield nothing worthwhile.

Instead of shifting the collocation points forward, the free surface source surface was

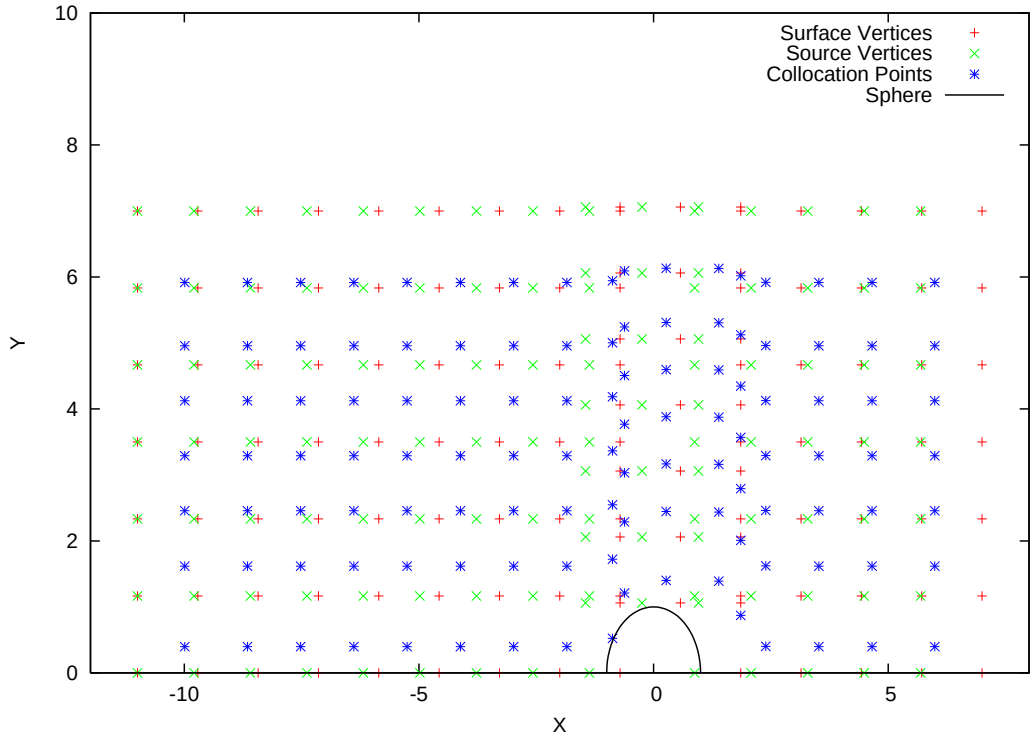

Figure 2.3: Free-surface source surface set-up

shifted downstream. The free surface source surface is an exact replication of the free surface, but, is situated slightly above the free surface in order to eliminate the singularity. The collocation points on free surface are within the boundaries of the free surface, ensuring that none lie exactly on the edge of the free surface. The source surface can only be shifted by shifting its vertices. The aft end of the source surface and the free surface originally lie on the same x-coordinate, and will remain like that even after the shift. Hence, the aft most vertices for both the surfaces are in line. Now each successive vertex on the source surface is moved aft by a distance that grows linearly as we move forward, until the forward most source surface vertex has been shifted aft by the maximum distance. Figure 2.3 clearly demostrates this linear aftward shift of the source surface. The important part is that the forward most vertex that undergoes the maximum aft shift has to be shifted enough to lie behind the forward most collocation point of the free surface. This set-up results in the desired wave-system downstream of the body.

Chapter 3

The Quasi-Singular Integral

The boundary element method in the current work is quasi-singular due to the presence of an inverse distance potential kernel. Potential flow problems may possess integrand of $O(1/r^3)$ for computing the surface integrals. For performing such numerical computations, it is imperative to depend upon numerical quadrature schemes [21]. As the distance r tends to zero, the kernel undergoes drastic changes in the function value. If the effect of the distance potential kernel is strong in the integrand, a large number of points are required to capture the true behavior of the function in the neighborhood of the singularity. Even then, standard integration methods generate large errors [13].

The integration method used is undisputably the backbone of any numerical procedure that deals with boundary element techniques. The efficiency and accuracy of the integration would make or break the overall performance of any such numerical procedure. One of the most effective methods that has been proposed to deal with a near singular boundary integral equation is element sub-division, followed by variable transformation [21] [14]. The coordinate transformation of an element generates a Jacobian that cancels out the singularity. Simply sub-dividing the element would pay-off, but intelligent concentration of points around the region of the weak singularity would avoid the reduction in the maximum degree of the allowable integrand [21]. Hence, a quadratic or cubic transformation is considered far more superior than a simple linear transformation. In order to truely appreciate the effectiveness of subdivision and transformation, it is worth discussing the problem first.

This section deals with the function values in the parametric domain, and therefore, it is necessary to look at the transformation of the body from the coordinate system defined in figure 1.1 to the parametric domain. Figures 3.1 and 3.2 show the transformation of a sphere and a Wigley hull into the parametric domain. The bottom end of the quarter of a sphere can be described by any value on the u coordinate, as long as the v coordinate is 0. For the wigley hull, the four corners have specific values in the u,v domain.

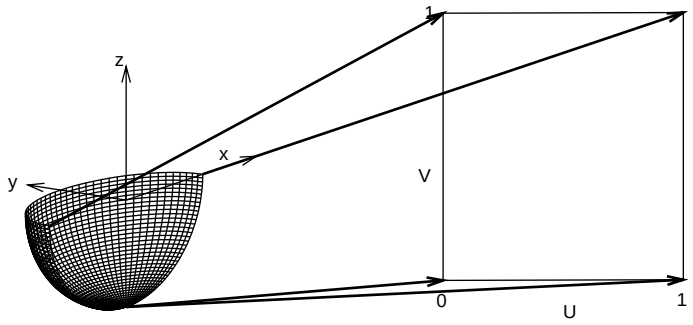

Figure 3.1: Transformation of a quarter of a sphere into the parametric domain.

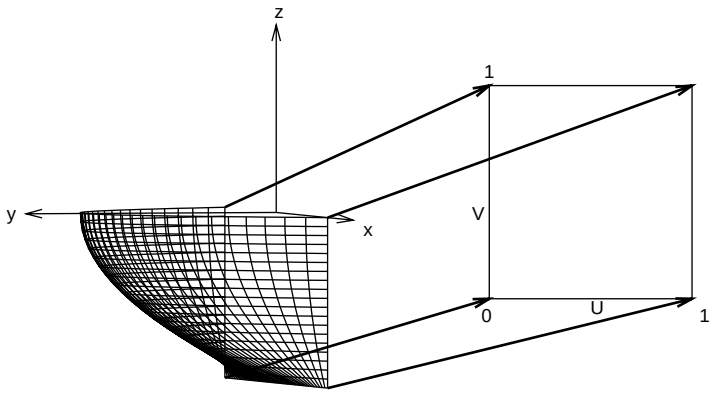

Figure 3.2: Transformation of a half Wigley hull into the parametric domain.

3.1 The Integrand

Figures 3.3, 3.4 and 3.5 represent the three velocity components of an original un-transformed source surface basis function. These components are for a source surface basis function of a sphere, which is subjected to a double body flow. These quasi-singular velocity components are the result of the effect of the source surface basis function under consideration, at a particular collocation point that lies within the same parametric limits as the source surface basis function. It is evident that even though most of the basis function is flat, in the vicinity of the collocation point it exhibits a drastic change in magnitude, over a small distance in the u and v directions.

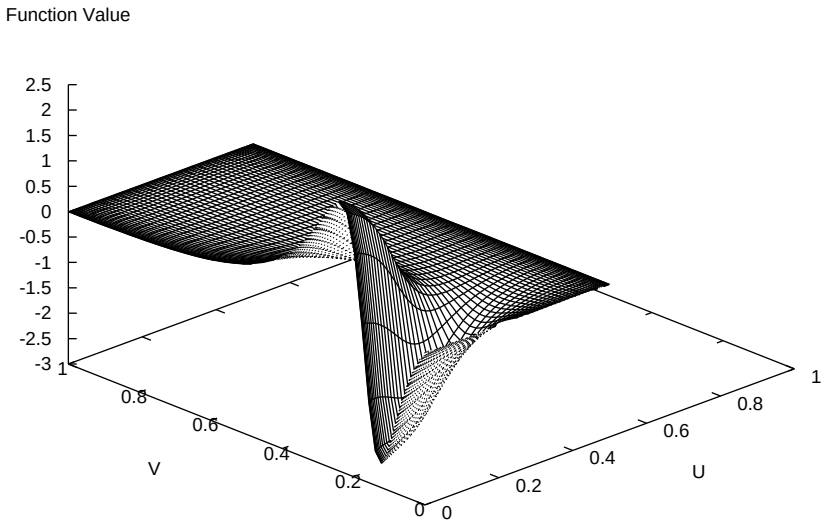

Figure 3.3: Original X component of the integral for double body flow around a sphere.

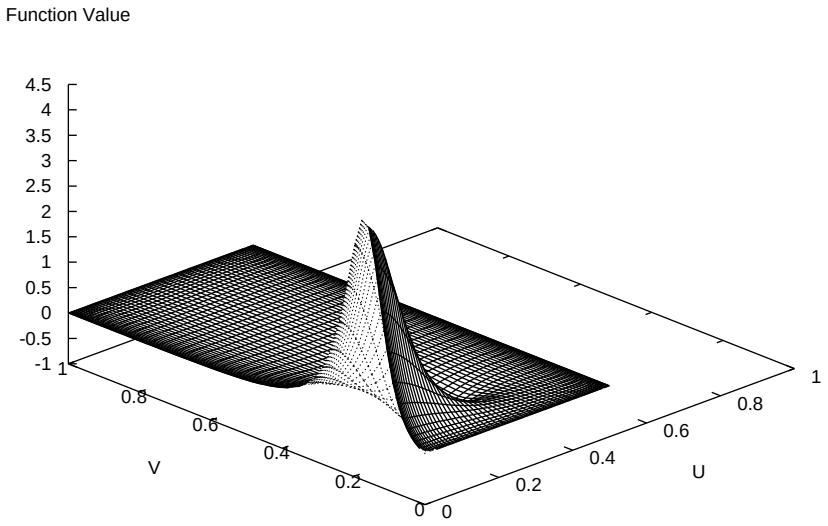

Figure 3.4: Original Y component of the integral for double body flow around a sphere.

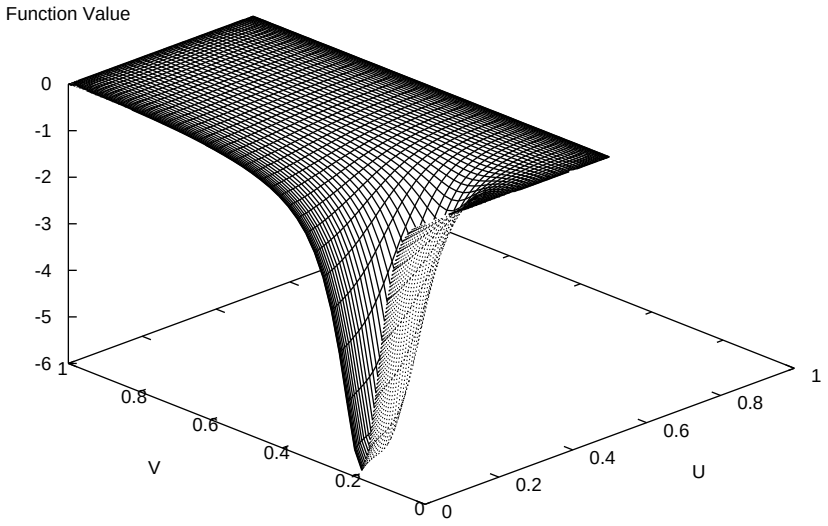

Figure 3.5: Original Z component of the integral for double body flow around a sphere.

An attempt to integrate the velocity components with a standard gaussian quadrature scheme is futile. Even though the singularity is nonexistent due to the shifting of the source surface, the drastic change in the values within a small distance on the parametric space makes integration a daunting task. Each source surface basis function would require a few hundred gaussian points before the results are considered accurate enough to be utilized in further numerical computations. Like all panel methods, we need to generate a square matrix. This would require the integration of a total of $N \times N$ source surface basis functions. Accurate integration of all these basis functions without compromising the overall computation time of the scheme is an unsurmountable task.

At first, dividing the surface into smaller sections seems to be a logical solution. Hence, separately integrating the almost flat region, and the region with quasi singular behavior. The former would require as few as 3×3 gaussian points. But since the velocity components are a function of the distance from the collocation point and the normal derivative of the potential, it is not a trivial task to accurately extract the region of singularity. Even if successfully separated, integrating this section would still be computationally expensive. In fact, the integration effort was noted to be almost the same as that required by the original undivided surface. Therefore, a more general technique is implemented that can be effectively executed for all cases. Though the solution still relies on surface sub-division, it is of a different kind.

3.2 Division and Transformation

The source surface is fundamentally a square in the parametric space. It is only in the global space that it attains the shape of the body. As the velocity components are a function of the distance between the source surface basis function and the collocation point, and the normal of the body surface at the collocation point, the quasi singular behavior is largely focused at the location of the collocation point. The square source surface is split into triangles based on the location of the peak of the velocity components [21] [14]. In Figure 3.6, the collocation point is assumed to be located at ε, hence, the source surface is divided into four triangular sub-elements. The apex of all the triangles is the location of the singularity. This basically subdivides the singular behavior of the source surface into smaller sections, therefore, making it less cumbersome to integrate. At this stage a common practice is to use a cylindrical coordinate system and integrate over these triangles [21]. Although less famous, an alternative to this is to re-transform these triangular sections back into squares. The transformation Jacobian thus employed helps in smoothing out the singularity that had existed in the triangles [14]. Instead of being linear, this transformation is quadratic. Hence, it helps to intelligently place the gaussian points, putting more points in the area where the original peak had existed.

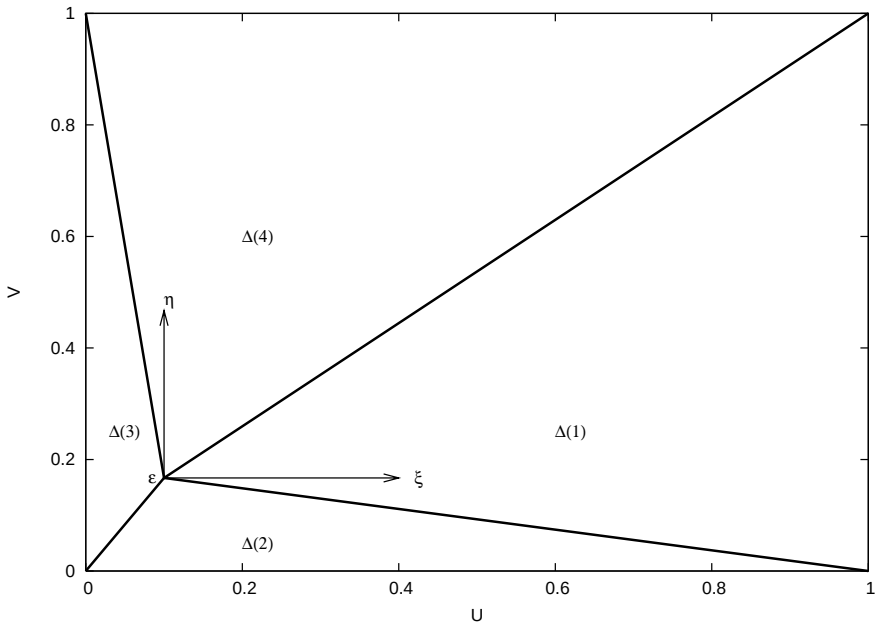

Figure 3.6: Element sub-division to eliminate the singularity [21].

Figure 3.7 shows the division of the Y component of velocity that was originally presented in Figure 3.4. Now the velocity effect on the source surface will be integrated in four separate parts. All the velocity components on all the source surfaces are split into triangles. The four traingles, thus obtained by division, are transformed back into a square.

Figure 3.8 is the transformation Jacobian for $\Delta(1)$. The Jacobian has really small values close to u=0. This is the region that lies near the apex of the triangle. The small value of the Jacobian helps in reducing the high function value, and smoothes the resulting surface in the square domain. The following expression is used to transform from the η and ξ domain to the u amd v domain. It is cubic in η, and linear in ξ.

$$u = \left((u_1 - u_p)\eta^3 + u_p\right)(1 - \xi) + \left((u_2 - u_p)\eta^3 + u_p\right)\xi \tag{3.1}$$

$$v = \left((v_1 - v_p)\eta^3 + v_p\right)(1 - \xi) + \left((v_2 - v_p)\eta^3 + v_p\right)\xi \tag{3.2}$$

where, u_p, v_p is the apex of the triangle. u_1, v_1 and u_2, v_2 are the coordinates of the other two corners. η and ξ represent the new domain after transformation.

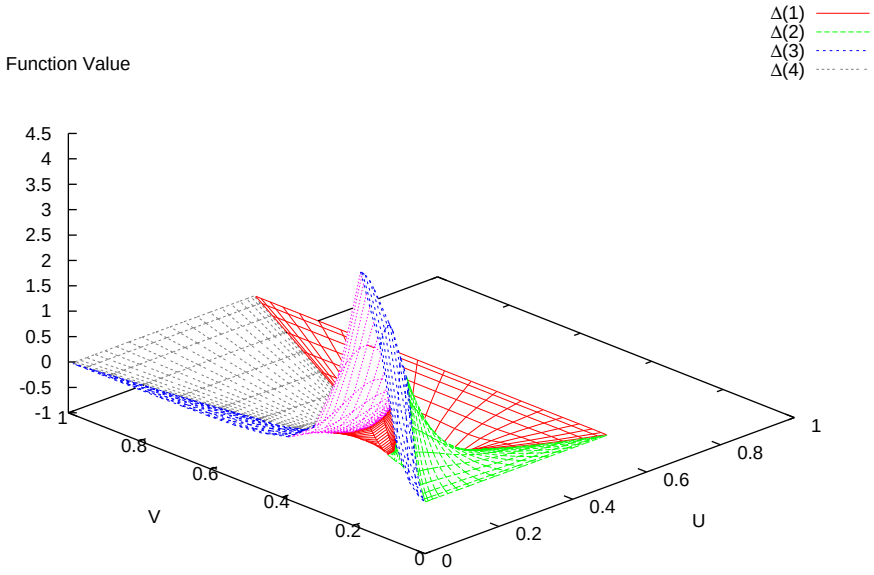

Figure 3.7: Surface sub-division of Y velocity component of a source surface for double body flow of a sphere.

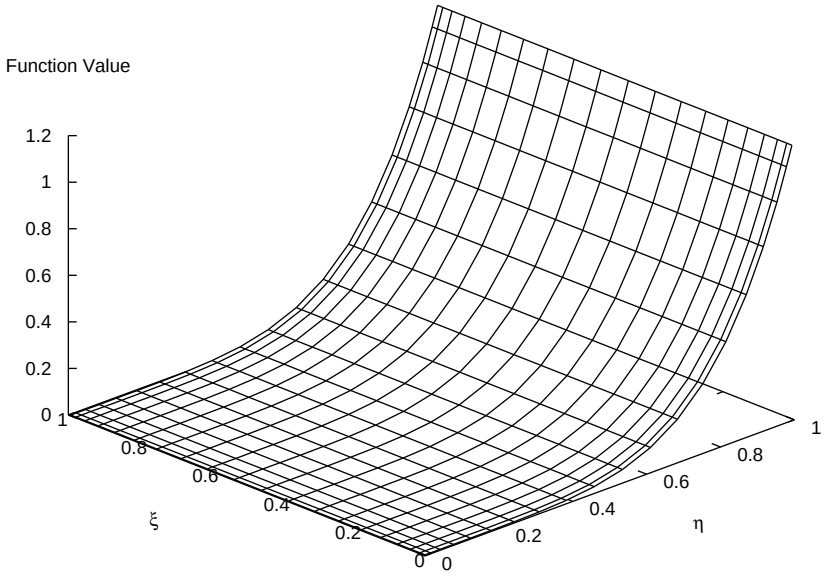

Figure 3.8: Transformation Jacobian for $\Delta(1)$

3.3 Effect of Division and Transformation

The Jacobian for each of the triangular section has the same smoothing effect. These newly obtained surfaces in the square domain can easily be integrated by using standard gaussian integration methods. And unlike previously, the divided and transformed components require much fewer guassian points. The figures on the following pages present the original Y components of all the triangular sections that were obtained after dividing the surface from figure 3.4, along with the surfaces that were obtained after performing the transformation.

It is evident from the figures that there has been a tremendous improvement in the irregularity of the surfaces that need to be integrated. We notice that after transformation, $\Delta(3)$ still exhibits the effect of the peak. It is worth pointing out that even though the peak has not been completely smoothed in $\Delta(3)$, the extent and the amplitude of the function value in the transformed surface has a great deal of improvement over the original $\Delta(3)$.

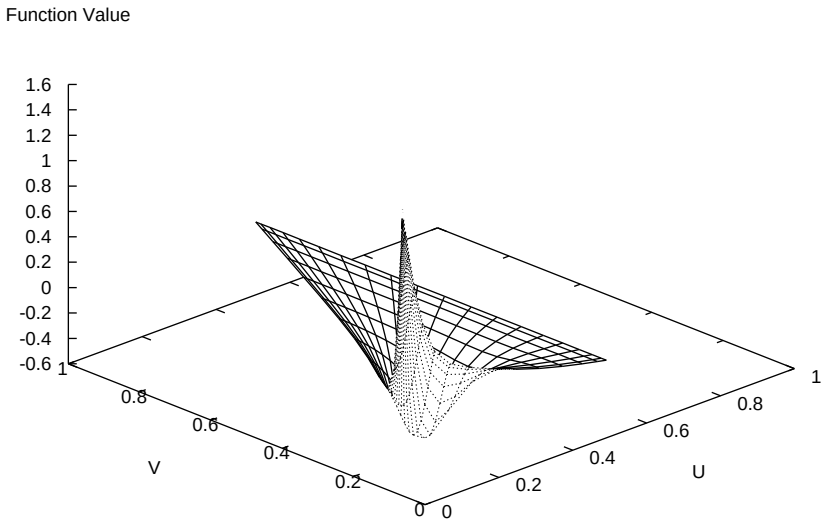

Figure 3.9: Original Y velocity component for $\Delta(1)$

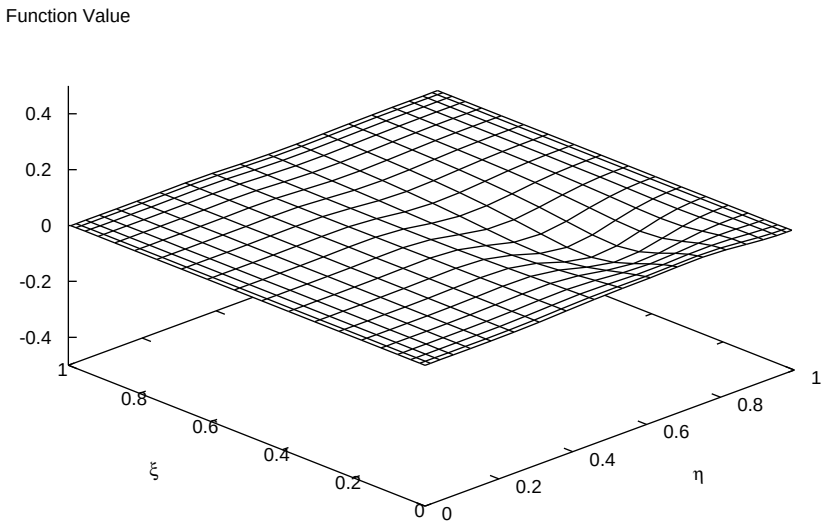

Figure 3.10: Transformed Y velocity component for $\Delta(1)$

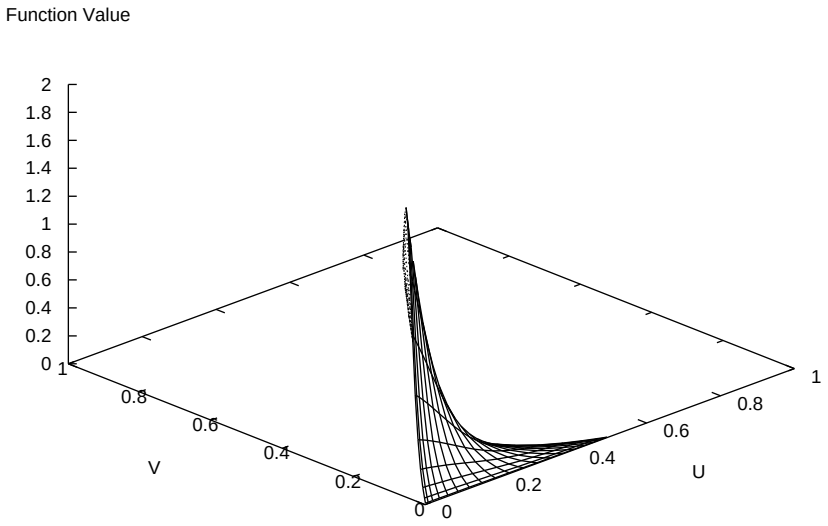

Figure 3.11: Original Y velocity component for $\Delta(2)$

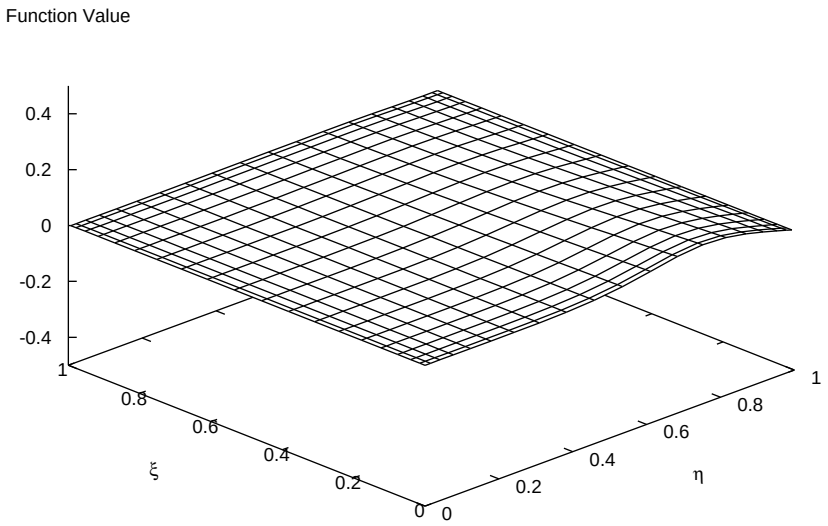

Figure 3.12: Transformed Y velocity component for $\Delta(2)$

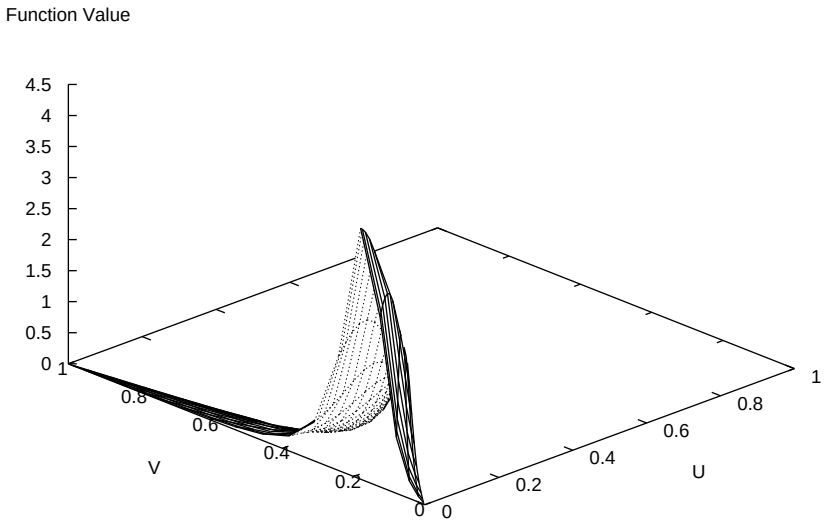

Figure 3.13: Original Y velocity component for $\Delta(3)$

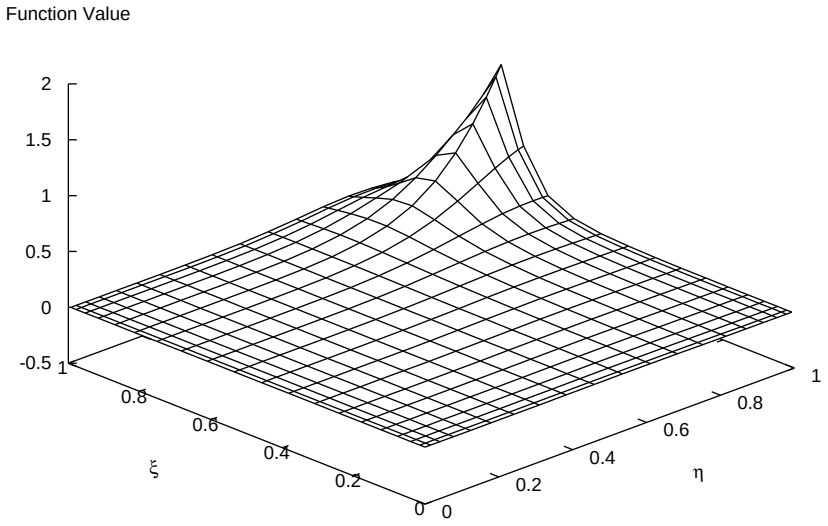

Figure 3.14: Transformed Y velocity component for $\Delta(3)$

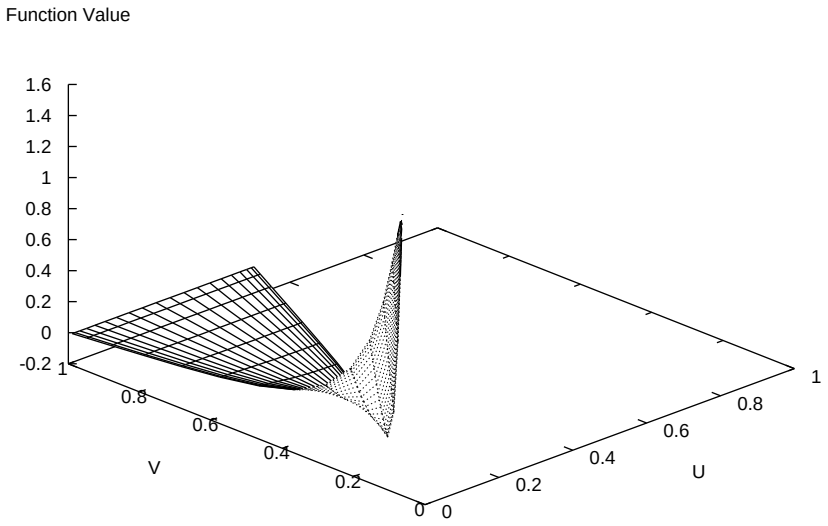

Figure 3.15: Original Y velocity component for $\Delta(4)$

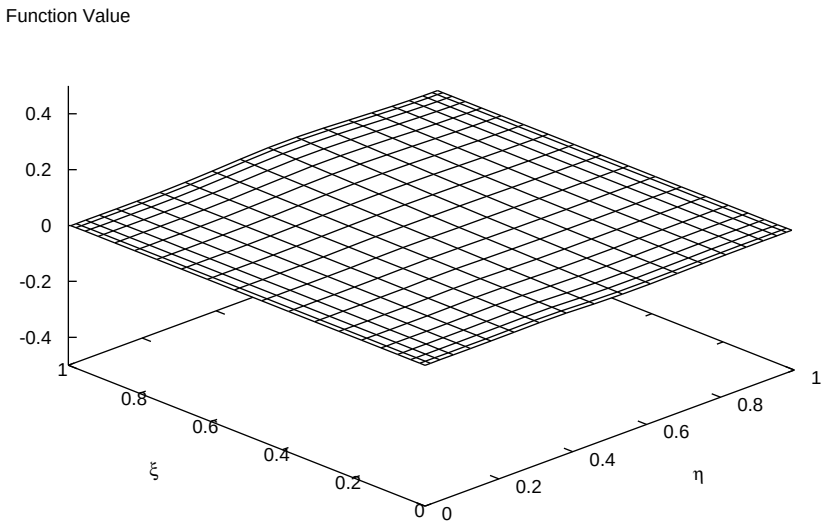

Figure 3.16: Transformed Y velocity component for $\Delta(4)$

Chapter 4

Results

The development of any numerical scheme in Naval Architecture, which is meant to solve the free surface flow problem, starts with the successful implementation of the same for the double body flow condition. Once accurate results are obtained for the double body flow case, the researcher is assured of the correctness of the basic formulation of the scheme. The same approach was used in the present work.

After the basic mathematical formulation was complete, the first milestone was achieved by solving the double body flow problem. A sphere and a Wigley hull were used to compare the results of the aforesaid case, with analytical and published data. Next, the task of implementation of the scheme to obtain the wave elevation in the presence of free-surface was undertaken.

This chapter summarizes the results for a sphere and a Wigley hull for both, double body and free-surface, conditions. Post processing of the results was done in Gnuplot (version4.0 - 2004) and Mayavi2.

4.1 Double Body Flow Problem

For a double body flow problem, the body is reflected about the free-surface, hence, supressing any waves that might be generated as a result of the fluid flow. The collocation points are only located on the body, where the body boundary condition needs to be satisfied. However, while satisfying the condition, the effect of another mirror image of the body, about the free-surface, is take into consideration.

4.1.1 Double Body Flow for a Sphere

The NURBS description of a quarter of a sphere is used to compute results for double body flow around a sphere. The symmetry of the body about the xz and xy planes allows us to reflect the quarter sphere about the two planes and generate a complete sphere.

The source distribution over the body, by itself, is not of much pratical use, but it will be beneficial to discuss all the different aspects of the results. Figure 4.1 is the source distribution over a quarter of a sphere for Fn=0.23. As mentioned in an earlier chapter, in the parametric domain, any point on the u coordinate, as long as the $v = 0$, is the same point on the sphere. As expected, the source value is same throughout u, for v=0. The net source value over the sphere is zero, hence, satisfying the total source requirement for a closed body. Also, the leading half of the quarter of a sphere has positive value, *source*, and the trailing half has negative value, *sink*.

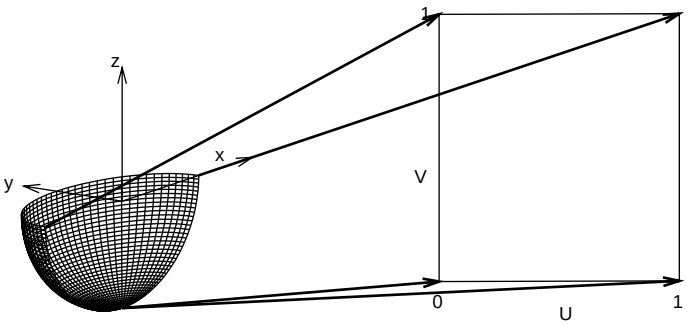

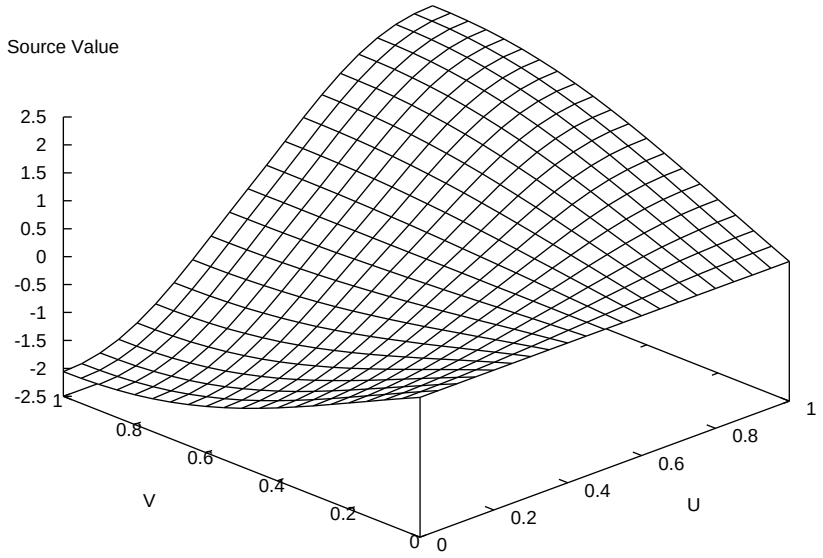

Figure 4.1: Source distribution for a quarter of a sphere with double body flow ($\alpha = 0.9$).

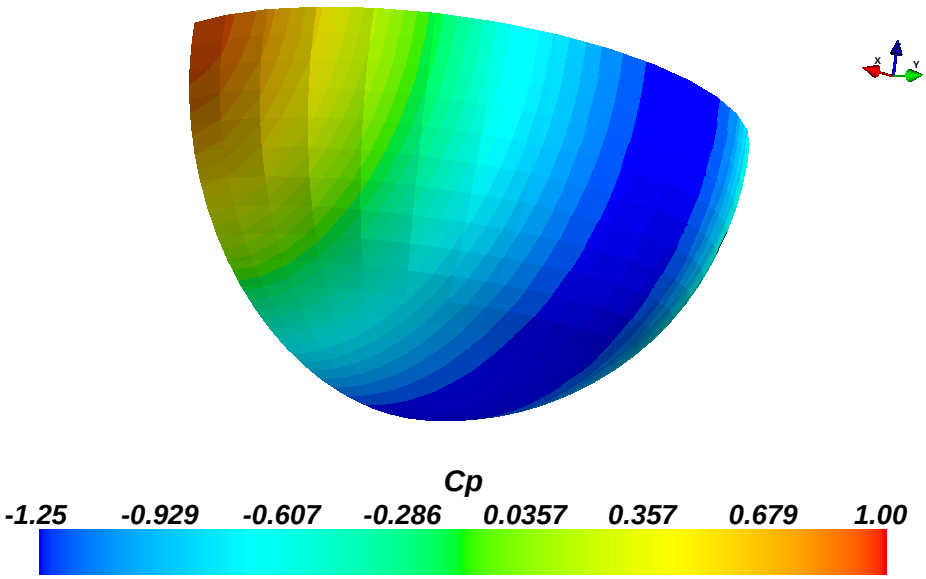

Figure 4.2: Cp for a sphere with double body flow ($\alpha = 0.9$).

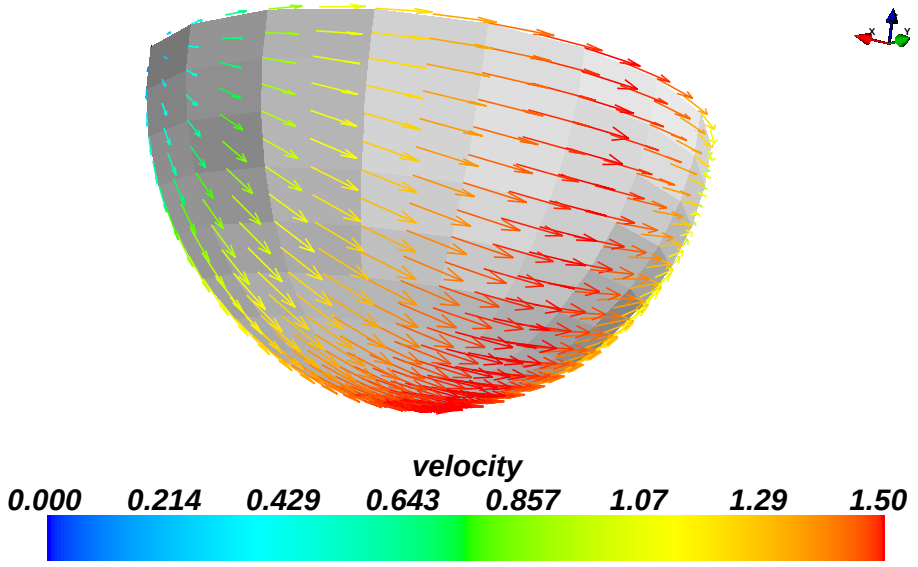

Figure 4.3: Velocity field on a sphere with double body flow ($\alpha = 0.9$).

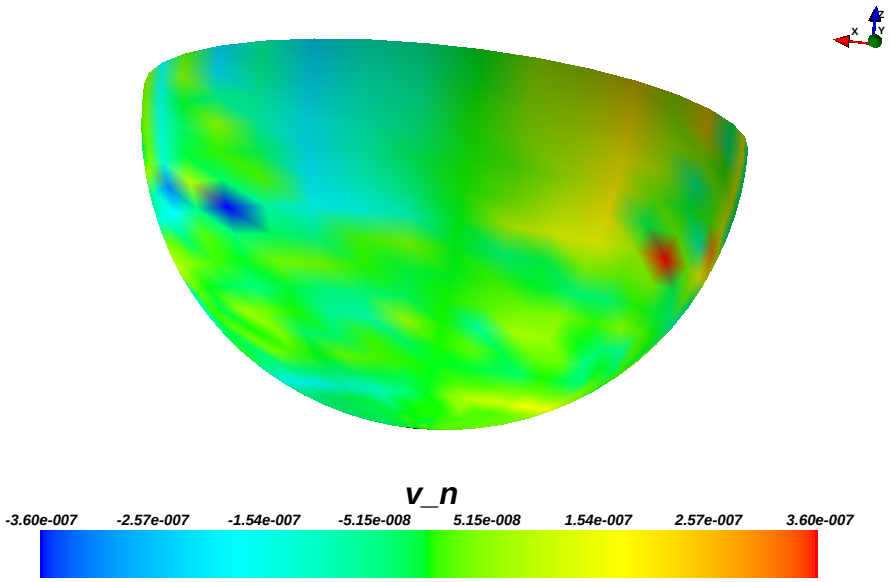

Figure 4.4: Normal velocity on a sphere with double body flow ($\alpha = 0.9$).

Figures 4.2 4.3 and 4.4 show the pressure distribution, velocity field and the normal velocity, respectively, for a sphere. The results agree with the analytical results for a sphere. Within the numerical precision, the normal velocity on the body surface is considered to be almost zero. Hence, satisfying the bounday boundary condition.

As the value for α is reduced, the source surface is moved away from the body surface. As the source surface moves away from the body surface the quasi-singular behaviour of the integral reduces. With the reducing α we don't see any change in the results. Figure 4.5 shows that there is no error in the pressure coefficient values as the source surface is moved away from the body surface. This is true for a sphere since its a simple shape, and all the points on the sphere surface is equidistant from the center. For a more complex geometry of the body we will have to maintain a high value of α to achieve accurate results.

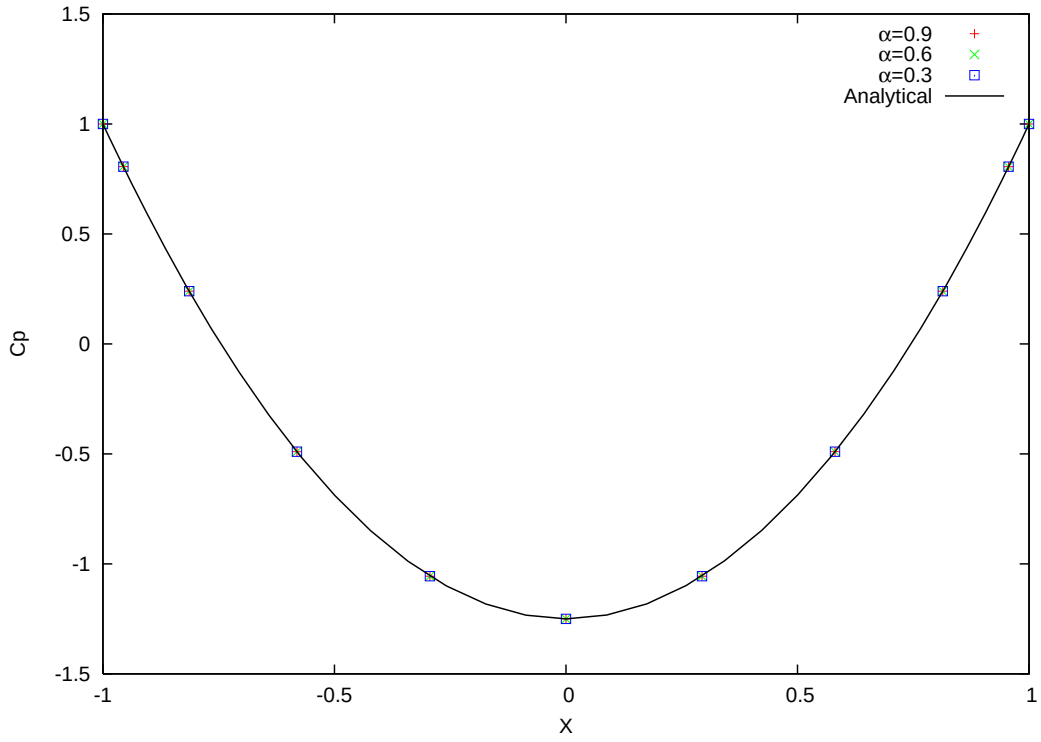

Figure 4.5: Comparison of C_p for different values of α with the analytical result for a sphere with double body flow. (values are at z=0 for a sphere of unit radius)

4.1.2 Double Body Flow for a Wigley Hull

The following are the results for a Wigley hull for a double body flow problem. Figures 4.6, 4.8 and 4.10 are the coefficient of pressure distribution over a Wigley hull that has been generated using 3×3, 4×3 and 4×4 surface vertices, respectively. We see an improvement in the values for the coefficient of pressure as the number of vertices is increased. Figures 4.7, 4.9 and 4.11 represent the velocity field over the Wigley hull. We can also see a change in the velocity field as the total number of vertices for the Wigley hull is increased. Remember, an increase in the number of surface vertices results in an increase in the number of collocation points too.

Figures 4.12 provides a better picture of the improving flow properties as we increase the number of surface vertices. The figure represents the pressure coefficient along the length of the Wigley hull at z = -1. We can see that the values converge as we increase the number of vertices.

Figure 4.13 shows the effect of changing the value of α. In the last section, the results did not change as we changed α for a sphere with double body flow. We had mentioned that this was due to the simple shape of a sphere. However, a Wigley is not a simple body like the sphere and is sensitive to the value of α. As we reduce the value of α, the change in pressure coefficient values at z=-1 for a 3×3 vertices Wigley hull is evident from figure 4.13.

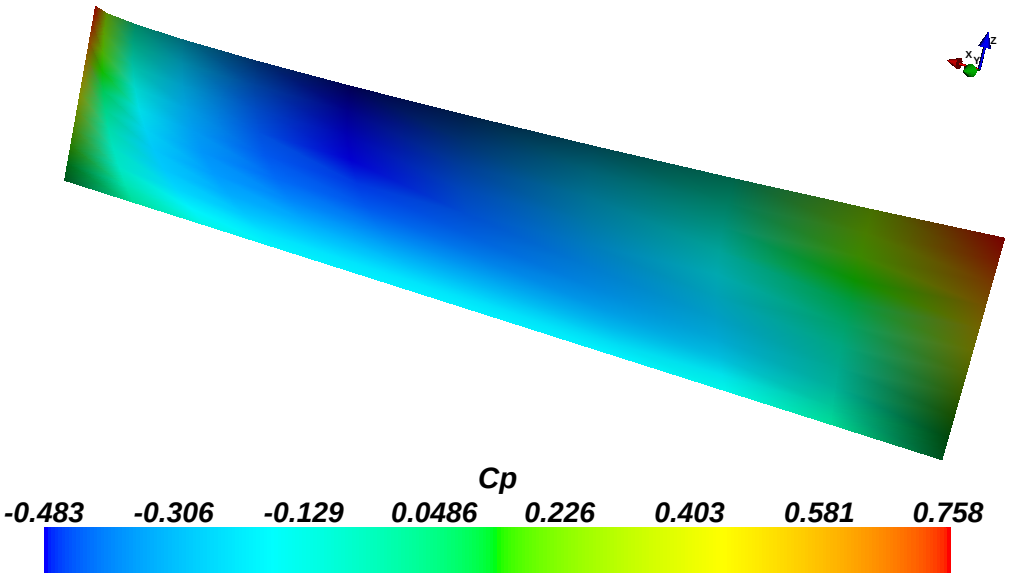

Figure 4.6: Cp for a Wigley hull with double body flow (3×3 vertices).

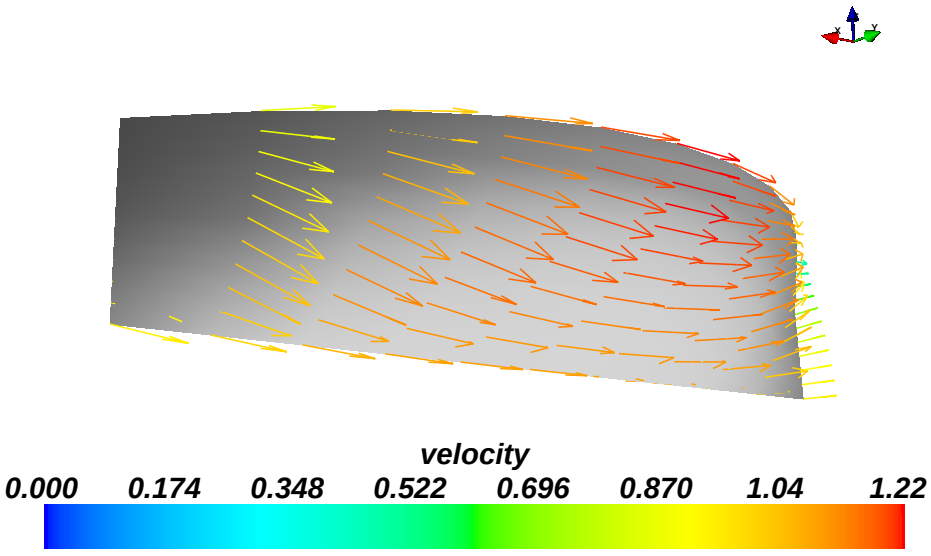

Figure 4.7: Velocity field on a Wigley hull with double body flow (3×3 vertices).

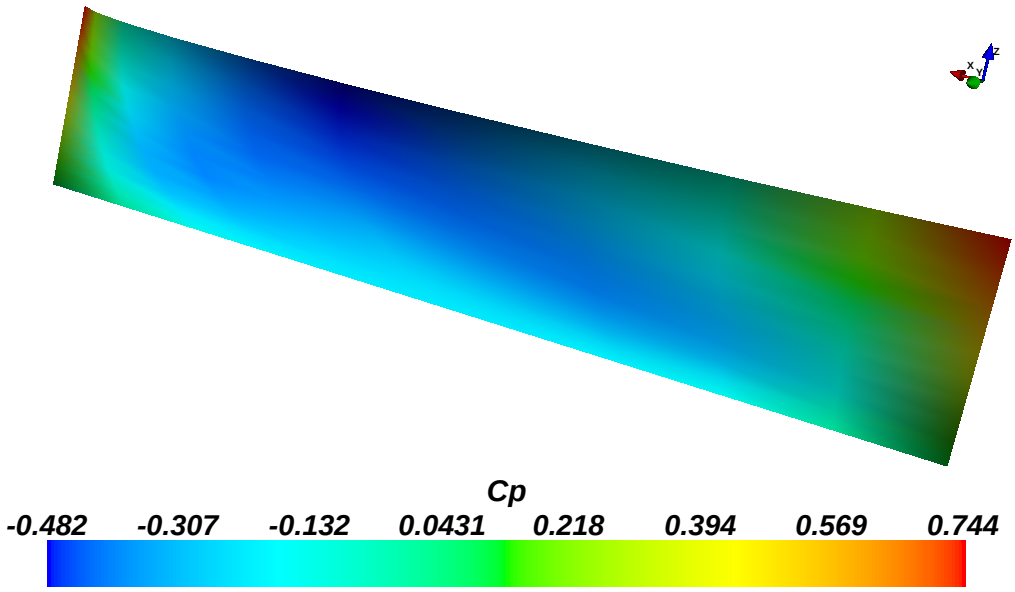

Figure 4.8: Cp for a Wigley hull with double body flow (4×3 vertices).

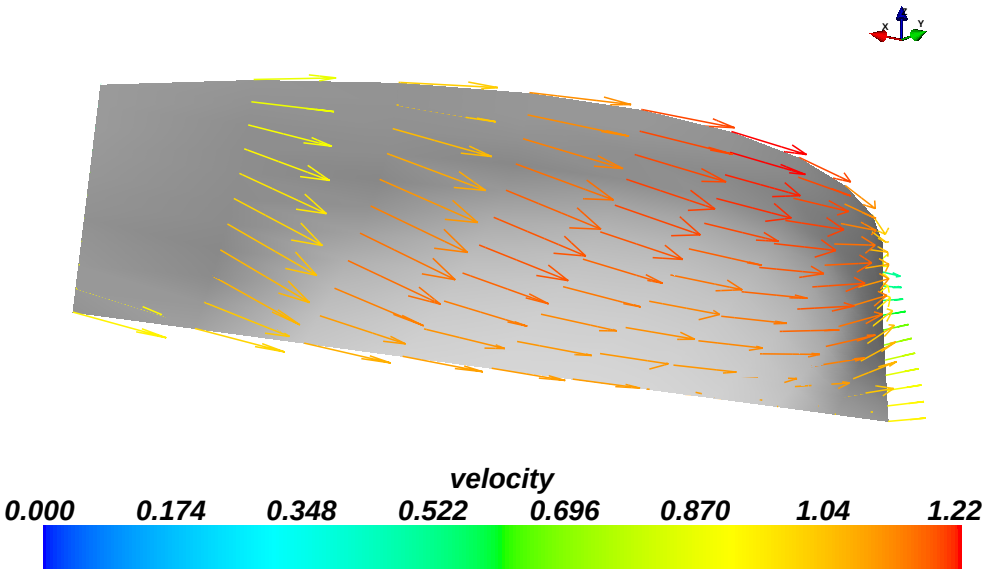

Figure 4.9: Velocity field on a Wigley hull with double body flow (4×3 vertices).

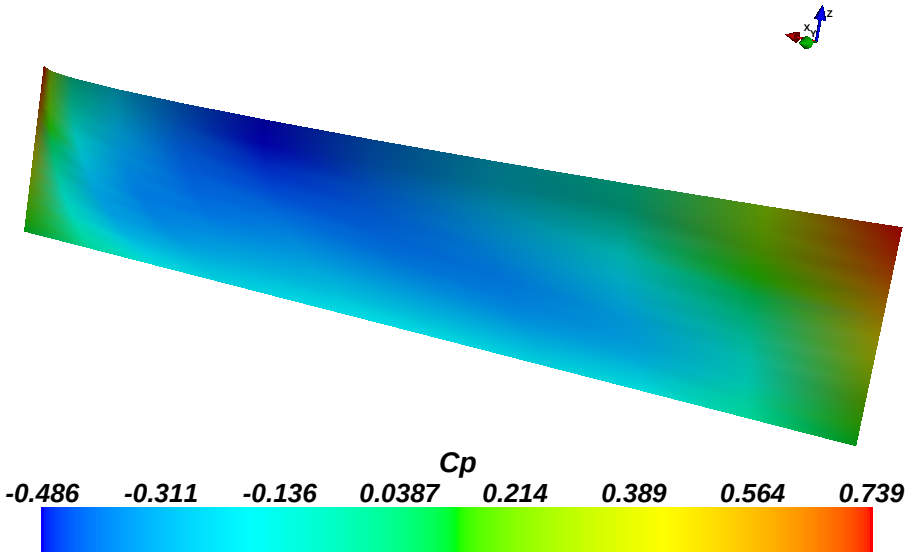

Figure 4.10: Cp for a Wigley hull with double body flow (4×4 vertices).

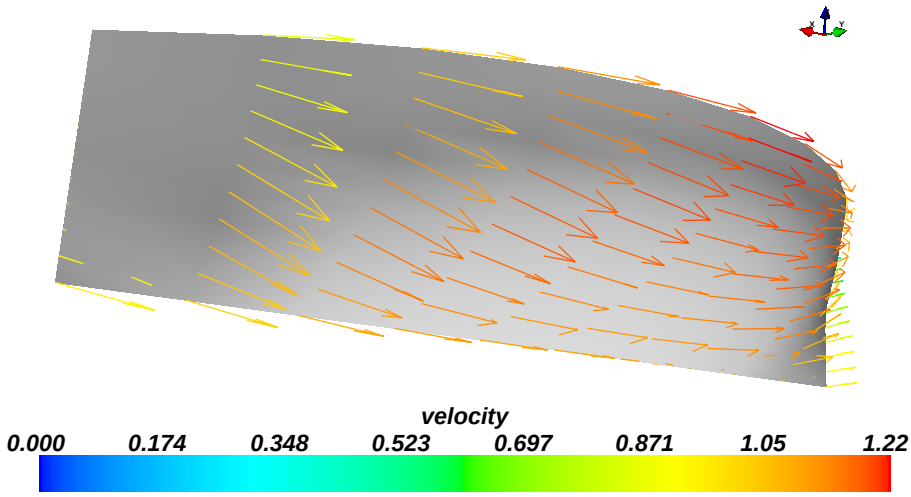

Figure 4.11: Velocity field on a Wigley hull with double body flow (4×4 vertices).

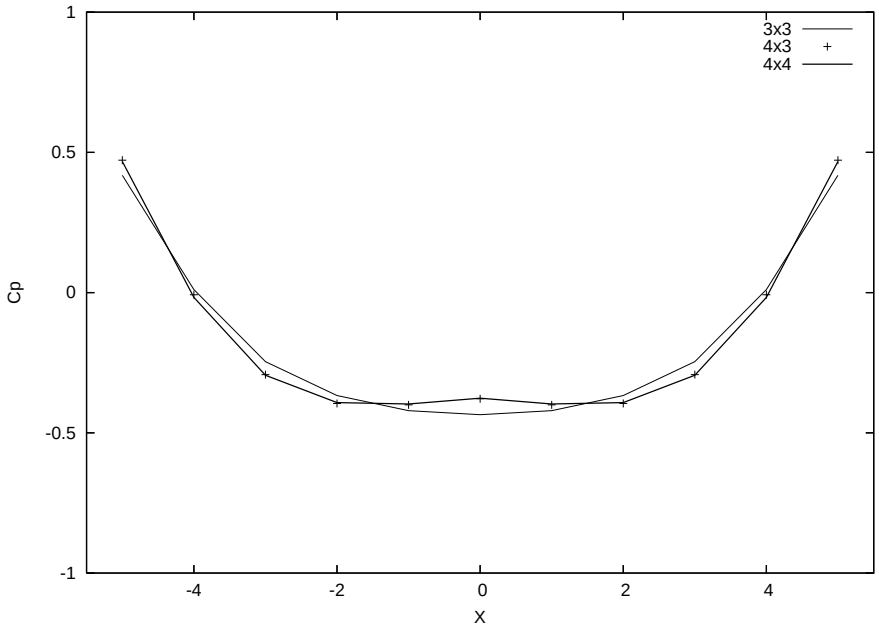

Figure 4.12: Cp for Wigley hull with different number of vertices for double body flow (at z = -1).

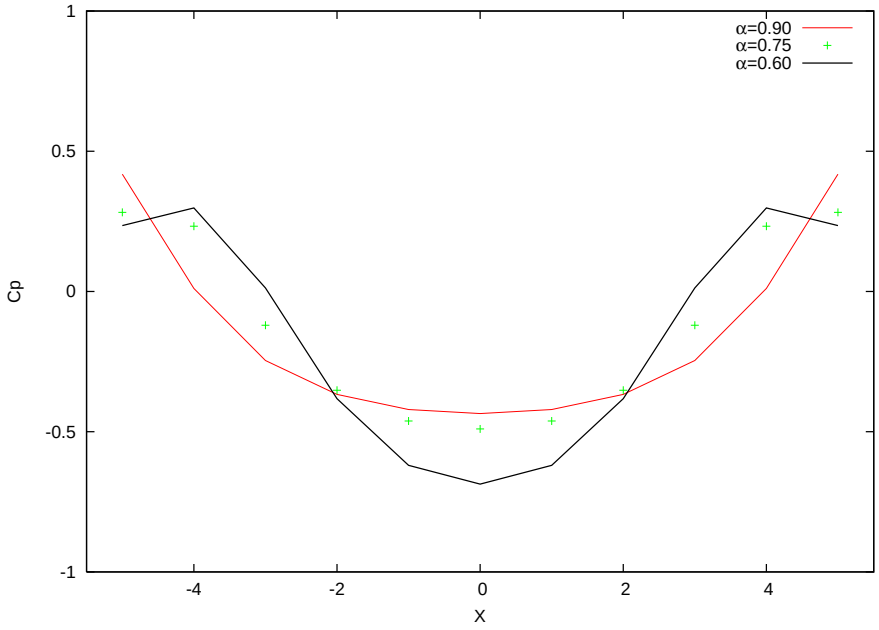

Figure 4.13: Cp for Wigley hull with varying α with 3×3 vertices for double body flow (at z = -1).

4.2 Linearized Free-Surface Problem

The results for the free surface problem are being refined. Preliminary result for a sphere is included in the following section.

4.2.1 Linearized Free-Surface For a Sphere

Figure 4.14 is the free surface elevation for a sphere.

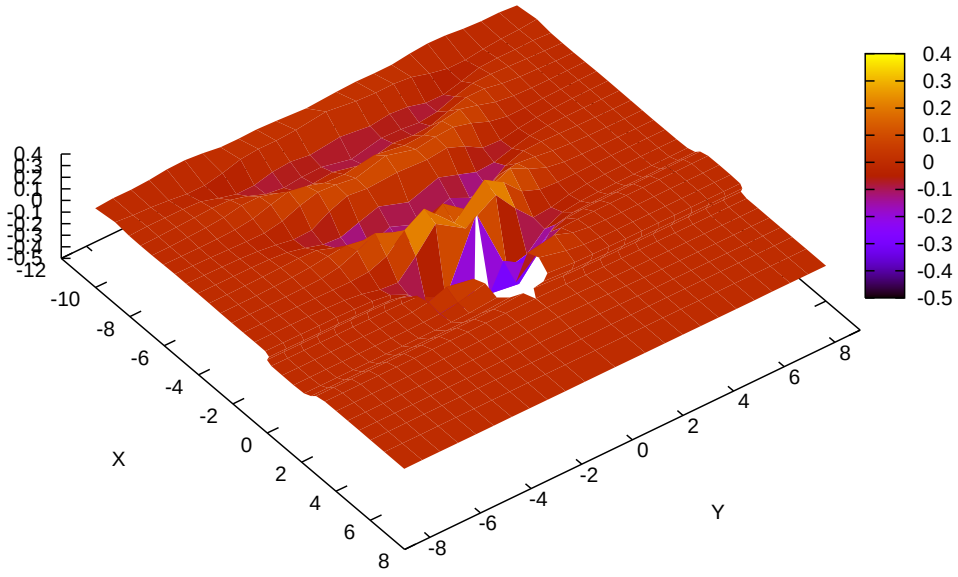

Figure 4.14: Free surface elevation for a sphere

Chapter 5

Conclusion and Future work

A novel method for potential flow analysis of bodies in the presence of free water surface is presented. The method uses a B-Spline source for the body surface, as well as the free water surface. The advantage of the high degree of continuity of the B-Spline functions allow the source surfaces to be exact, instead of being panels or points. The technique successfully solves double body flow and linear free surface condition problems. The use of a separate and single B-Spline source for the free water surface, instead of a free surface Green's function, allows extendibility of the method to solving non linear free surface conditions as well.

The obvious advantages include the availability of the exact derivatives of the basis functions for the B-Spline surface, hence, eliminating the need for numerical schemes to differentiate. And, a much smaller system matrix than the constant panel method. Once the values of the source strength vertices have been computed, the method allows complete flexibility of computing the fluid properties at any arbitrary point on the body surface or the free surface. In comparison, the constant panel method restricts the computation to the collocation points. The B-Spline for the surfaces can be of any order, hence, the solution can possess any order. Due to lack of actual panels, utilization of the method for external wave forcing problems will mitigate, or might even fully eliminate, the irregular frequency problem.

The results that have been presented in this work agree with the analytical and benchmark results. The current work provides another approach to solving the steady-state ship wave-resistance problem in marine hydrodynamics. For solving the wave resistance problem it is necessary to satisfy the non-linear free surface conditions. And the success in solving the linear free surface conditions has paved way to proceed with an attempt to solve the non-linear free surface conditions in the near future. The solution to the non-linear free surface conditions would hence allow successful computation of wave resistance for existing and new ship hull designs.

Bibliography

[1] K.E. Atkinson. *Numerical Solution of Integral Equations*, volume 42, chapter A survey of boundary integral equation methods for the numerical solution of Laplaces equation in three dimensions, pages 1–34. Plenum, 1990. 5

[2] S. Bal. A numerical method for the prediction of wave pattern of surface piercing cavitating hydrofoils. *Mechanical Engineering Science*, pages 1623–1633, 2007. 20, 24

[3] L. Birk. Numerical methods in hydrodynamics (name 6160) class notes. University of New Orleans, Fall 2006. 4, 19, 24

[4] Ranadev Datta and Debabrata Sen. A b-spline-based method for radiation and diffraction problems. *Ocean Engineering*, 33:2240–2259, 2006. 1, 6

[5] C.W. Dawson. A practical computer method for solving ship-wave problems. In *International Conference on Numerical Ship Hydrodynamics*, volume 2nd, pages 30–38. University of California, Berkeley, 1977. 6, 20, 24

[6] J.L. Hess. A higher order panel method for three-dimensional potential flow. Technical report, Douglas Aircraft Co., Inc, 1979. 6

[7] John L. Hess and A.M.O. Smith. Calculation of non-lifting potential flow about arbitrary three-dimensional bodies. Technical Report E. S. 40622, Douglas Aircraft Co., Inc, March 1962. 2, 6

[8] C.Y. Hsin, J.E. Kerwin, and J.N. Newman. A higher order panel method based on b-spline. In *Proceedings of the Sixth International Conference on Numerical Ship Hydrodynamics*, volume 6, pages 133–151. National Academy Press, 1994. 6

[9] G. Jensen. Berechnung der stationaeren potentialstroemung um ein schiff unter beruecksichtigung der nichtlinearen randbedingung an der wasseroberflaeche. Technical Report IfS-Report 484, University of Hamburg, 1988. 24

[10] F.T. Johnson. A general panel method for the analysis and design of arbitrary configuration in incompressible flows. NASA contractor report 3079, National Aeronautics and Space Administration, 1980. 6

[11] Joseph Katz and Allen Plotkin. *Low-Speed Aerodynamics*. Cambridge University Press, 2 edition, 2001. 2, 4

[12] Y.Z. Kehr, C.Y. Hsin, and Y.C. Sun. Calculations of ship surface force induced by intermittently cavitating propellers using simplified free surface boundary condition. In *9th Conference on SNAME ROC*, pages 379–397, 1996. 6

[13] Roland Klees. Numerical calculation of weakly singular surface integrals. *Journal of Geodesy*, 70:781–797, 1996. 27

[14] Yin-Sheng Li, Tatsuo Obata, Hideo Koguchi, and Toshio Yada. Some improvements of accuracy and efficieny in three dimensional direct boundary element method. *International Journal for Numerical Methods in Engineering*, 33:1451–1464, 1992. 27, 33

[15] Hiren Dayalal Maniar. *A three dimensional higher order panel method based on B-splines.* PhD thesis, Massachusetts Institute of Technology, September 1995. 6

[16] J.N. Newman. *Marine Hydrodynamics.* The MIT Press, Cambridge, Massachusetts, 1977. 1, 4, 19

[17] H. Nowacki, J. Michalski, B. Oleksiewicz, M.I.G. Bloor, C.W. Dekanski, and M.J. Wilson. *Computational Geometry for Ships.* World Scientific, 1995. 9

[18] Les Piegl and Wayne Tiller. *The NURBS Book.* Springer-Verlag, New York, NY, 2nd edition, 1997. 9

[19] P.D. Sclavounos and D.E. Nakos. Stability analysis of panel methods for free-surface flows with forward speed. In *Seventeenth Symposium on Naval Hydrodynamics*, pages 173–193. National Academy Press, 1989. 6, 20

[20] Jen shiang Kouh and Jyh bin Suen. A 3d potential-based and desingularized high order panel method. *Ocean Engineering*, 28:1499–1516, 2001. 6

[21] J.C.F. Telles. A self-adaptive co-ordinate transformation for efficient numerical evaluation of general boundary element integrals. *International Journal for Numerical Methods in Engineering*, 24:371–381, 1987. vi, 27, 33, 34

[22] Ronald W. Yeung. Numerical methods in free-surface flows. *Annual Review of Fluid Mechanics*, 14:395–442, 1982. 19, 24

Vita

Aditya Mohan Aggarwal, born in Delhi, India, obtained a Diploma in Marine Engineering (Marine Power Plant) from Singapore Polytechnic in 2000, where he was the top graduate of his class. From 2001 to 2004, he served with American President Lines as an Engineering Officer onboard their merchant container fleet. He graduated Magna Cum Laude in August 2006 from the University of New Orleans, New Orleans, Louisiana, with a Bachelors (Honors) degree in Naval Architecture and Marine Engineering. He will be joining **American Bureau of Shipping Americas**, and will be working as a Naval Architect in the Offshore Engeering Department.